3-1-1999

A Systematic study to investigate the effect of concentration on flow boiling heat transfer characterisics in water ethylene glycol system

Murat Bulut

A SYSTEMATIC STUDY TO INVESTIGATE THE EFFECT OF CONCENTRATION ON FLOW BOILING HEAT TRANSFER CHARACTERISTICS IN WATER ETHYLENE GLYCOL SYSTEM

Murat Bulut

Mechanical Engineering Department
Rochester Institute Of Technology
Rochester, NY

A Thesis Submitted
in
Partial Fulfillment
of the
Requirements for the

MASTER OF SCIENCE

in

Mechanical Engineering

Approved by:

Professor_____
Dr. S. Kandlikar, Thesis Advisor

Professor_____
Dr. A. Ghosh

Professor_____
Dr. A. Nye

Professor_____
Dr. C. Haines, Department Head

PERMISSION TO REPRODUCE

Thesis Title: "A Systematic Study to Investigate the Effect of Concentration on Flow Boiling Heat Transfer Characteristics in Water Ethylene Glycol System."

I, Murat Bulut, hereby grant permission to the Wallace Memorial Library of the Rochester Institute of Technology to reproduce my thesis in whole or part. Any reproduction can not be used for commercial use or profit.

MARCH 1999

PERMISSION TO REPRODUCE

Thesis Title: "A systematic study to investigate the effect of concentration on flow boiling heat transfer characteristics in water ethylene glycol system."

I, Murat Bulut, hereby grant permission to the Wallace Memorial Library of the Rochester Institute Of Technology to reproduce my thesis in whole or part.

Any reproduction can not be used for commercial use or profit.

March, 1999

FORWARD

I wish to express my appreciation to my thesis advisor, Dr. Satish Kandlikar. He has taught me the value of being relentless in approaching my challenges. To him, I am forever grateful.

Also, I would like to thank to my uncle, Alaattin Bulut and MY FAMILY, who sponsored my MS program in USA. Similarly, my special gratitude goes to Department Head, Dr. Charles Haines, for keeping my hopes alive to endure this program.

This great work would not be complete, however, without mention and without expression of my appreciation to the following people.

- Paul Spiesman for helping me start my thesis in 1997 summer.
- Ryan Fogarty for being a friend of mine, but especially for helping me whenever I needed him.
- Ronald Hamaoui and Michael Moorhead for helping me whenever I had a problem with the computer.
- Tom Locke, Jim Greanier, Dave Hathaway
- The crew in the Thermal Lab, Dominic Peters, Lucas Carvalho Alves.
- James Wentworth for helping my English.
- The ladies in the mechanical engineering office.

Abstract

Mixtures of ethylene glycol and water are employed in cooling engines in automotive applications. To avoid two-phase flow in the engine, the mixture is subcooled in the radiator before entering the engine block. Heat transfer is therefore essentially under subcooled flow boiling conditions. Very little information is available in the literature on the subcooled flow boiling (flow boiling with subcooled liquid) characteristics of this mixture and there are no predictive methods established in this region.

In the present investigation heat transfer in the nucleate flow boiling of dilute aqueous binary mixtures was measured and experimental data were compared with available correlating methods developed for binary mixtures. The concentration range from pure water to 40 percent ethylene glycol solution is tested under these conditions. Eighteen different concentrations have been investigated. Liquids were boiled at atmospheric pressure on a rectangular flow channel. The experimental set up consists of a 9.5 mm circular heater placed on the lower wall of a 3 mm x 40 mm horizontal channel.

The results indicate that increasing the concentration of ethylene-glycol in water deteriorates the heat transfer coefficients as compared to the case of pure water at the same wall superheat.

TABLE OF CONTENTS

NOMENCLATURE

A_{12}	Thermodynamic factor
A_C	Cross sectional area
a	Thermal diffusivity of bulk liquid
Bo	Boiling number, $=q/(G\Delta h_{lg})$
C	Chord length
c	Mass specific heat of bulk liquid
c_p	Specific heat, J/kgK
Co	Convection number, $=(\rho_G/\rho_L)^{0.5}((1-x)/x)^{0.8}$
D	Diameter of tube, m /Mass diffusivity of bulk liquid, diameter
D_h	Hydraulic diameter, mm
D_{12}	Diffusion coefficient 1 in mixture of 1 and 2
D_{12}^0 and D_{12}^0	Diffusion coefficient of component 1 present in infinitely low concentration of liquid mixture
f	Friction factor
F_D	Diffusion factor, $=\alpha/\alpha_{id}$
F_{fl}	Fluid-surface parameter
Fr_{lo}	Froude number with all flow as liquid$=G^2/(\rho_L^2 gD)$
G	Mass flux, kg/m^2 s / Vaporized mass diffusion constant
g-$=(x_1-x_{1,s})/(y_{1,s}-x_{1,s})$	Liquid-vapor mass fraction ratio
Δh_{LG}	Latent heat of vaporization, J/kg
Ja_0	Modified Jakob number, defined by eq.(2.12)
P	Pressure
Pr	Prandtl number, $c_p\eta/\kappa$

q	Heat flux, W/m^2
R, r	Bubble radius
Re	Reynolds number, GD/η
Re_L	Liquid Reynolds number $=GD(1-x)/\mu_L$
S	Bubble growth rate suppression factor
T	Temperature, K
ΔT_s-=(T_s-T_{sat}), K	
t	Time
$v_{m,1}, v_{m,2}$	Molar specific volume 1 and 2, m^3/kg-mol
V_1	Volatility parameter, defined by eq.(2.10)
x	Quality
x_1, x_2	Mass fraction of components 1 and 2 in liquid phase
X	Volume fraction of ethylene glycol
X_1	Mole fraction of more volatile component in liquid phase
X_V	The bulk vapor concentrations of the more volatile component
Y	Volume fraction of water
Y_1	Mole fraction of more volatile component in vapor phase
y_1, y_2	Mass fraction of components 1 and 2 in vapor phase
x_1^-, x_2^-	Mole fraction of components 1 and 2 in liquid phase

Greek Letters

α	Heat transfer coefficient, W/m^2K
η	Viscosity, kg/m s
κ	Thermal diffusivity, m^2/s

λ	Thermal conductivity, W/m K
ρ	Density, kg/m^3
σ	Surface tension, N/m
ϕ	Association number

Subscripts

1,2	Components of a binary system, 1-more volatile component
B	Binary
CBD	Convective boiling dominant
D	Mass diffusion
G	Vapor
id	Ideal
L	Liquid
LO	Entire flow as liquid
M	Mixture
NBD	Nucleate boiling dominant
PB	Pool boiling
Psc	Pseudo-single component
S	Liquid-vapor interface of a bubble
Sat	Saturation
TP	Two-phase

LIST OF FIGURES

LIST OF TABLES

1. Introduction

Boiling heat transfer can be classified as pool boiling and flow boiling. Although pure liquids are encountered in many applications, there are a number of areas where mixtures are employed in processes involving phase change. For example, petrochemical and chemical industries employ such mixtures. Another application is engine cooling using mixtures of ethylene glycol and water. Nucleate pool boiling of binary mixtures has been extensively investigated over the last six decades. On the other hand, flow boiling has received little attention in the past even though flow boiling applications can be found in the heating, air conditioning, process, oil refinery, nuclear power, automotive, and energy conversion systems.

Nucleate boiling occurs in pool boiling and flow boiling as mentioned above. In pool boiling, the fluid is not forced to flow by a mover such as a pump, and any motion of the fluid is due to natural convection and the motion of the bubbles under the influence of buoyancy. A familiar example of pool boiling is the boiling of water in a pan on the top of a stove. In flow boiling, the fluid is forced to move by an external source such as a pump as it undergoes a phase-change process. In this case, heat is transferred by forced convection.

Binary fluid mixtures are basically mixtures of two pure fluids. The mixtures of these two fluids have different saturation temperature at different concentration. Thermodynamic and thermophysical properties of binary mixtures

are different than the respective pure fluids (i.e density, viscosity, etc) and therefore will have different heat transfer coefficient than pure water or pure ethylene glycol in our case of study. The microscopic bubbles that form will also have different properties such as growth rate, contact angle, and departure bubble diameter.

Experimental work has been done in the present investigation with binary mixtures of ethylene glycol -water solutions. A wide variety of flow rates, concentrations and temperatures have been tested.

The experimental results generated in this work are believed to be useful in designing engine cooling systems in automotive applications.

2. LITERATURE REVIEW

There are fewer studies available in the literature on the flow boiling heat transfer compared to the pool boiling of binary mixtures. Before discussing the nucleate flow boiling of binary mixtures, the following sections will describe some of the basic aspects of flow boiling with binary mixtures.

2.1 Binary mixtures

Boiling of binary mixtures is a complex process influenced by the mass diffusion of the more volatile fluid toward the liquid-vapor interface of a nucleating bubble. This results in a change in interface saturation temperature with time during the bubble growth cycle. Boiling curves, q" versus ΔT, for mixtures lie between the respective curves for the two pure components.

2.2 Boiling Heat transfer

There are two types of boiling: *pool boiling* and *flow boiling* as mentioned previously.

Pool boiling occurs in the absence of bulk fluid flow, such as in the boiling of a pan of water. This kind of boiling can be produced by submerging an electrically heated wire in a pool of liquid.

Flow boiling processes occur in industrial equipment such as nuclear steam generators and refrigerant evaporators. Efficient heat transfer in this type of equipment are important from energy saving viewpoint.

Pool and flow boiling are also classified according to the bulk-liquid temperature which may be equal to or less than the saturation temperature. If the bulk temperature of the liquid is less than T_{sat}, the process is called as *subcooled boiling*. If the bulk temperature of the liquid is higher than T_{sat}, the process is called as *saturated boiling*.

Before discussing flow boiling with binary mixtures, first a discussion on flow boiling of pure components and the characteristics of binary mixtures are discussed in the following subsections.

2.3 Flow Boiling

In flow boiling, liquid or liquid-vapor mixture enters a heated channel as subcooled liquid. Following the onset of nucleation at a certain location is the quality of the liquid-vapor mixture increases with distance until total vaporization occurs. Therefore, the bulk-fluid temperature increases to the value somewhat less than T_{sat} , at which nucleate boiling is started. The bulk temperature quickly reaches with T_{sat} further addition of heat, the quality goes from zero to one as the liquid is completely evaporated along the length of the evaporator tube. Further heat addition results in superheating of the vapor.

2.3.1 Boiling curve for flow boiling

A boiling curve for flow boiling in heated tubes and channels is shown in Fig.(2.1). It can be seen from Fig.(2.1) that with the wall superheat ΔT_{sat} represented by T_w-T_{sat} for internal flow, the boiling curve for pool boiling and flow boiling are of the same general form. Points on the flow boiling curve show the

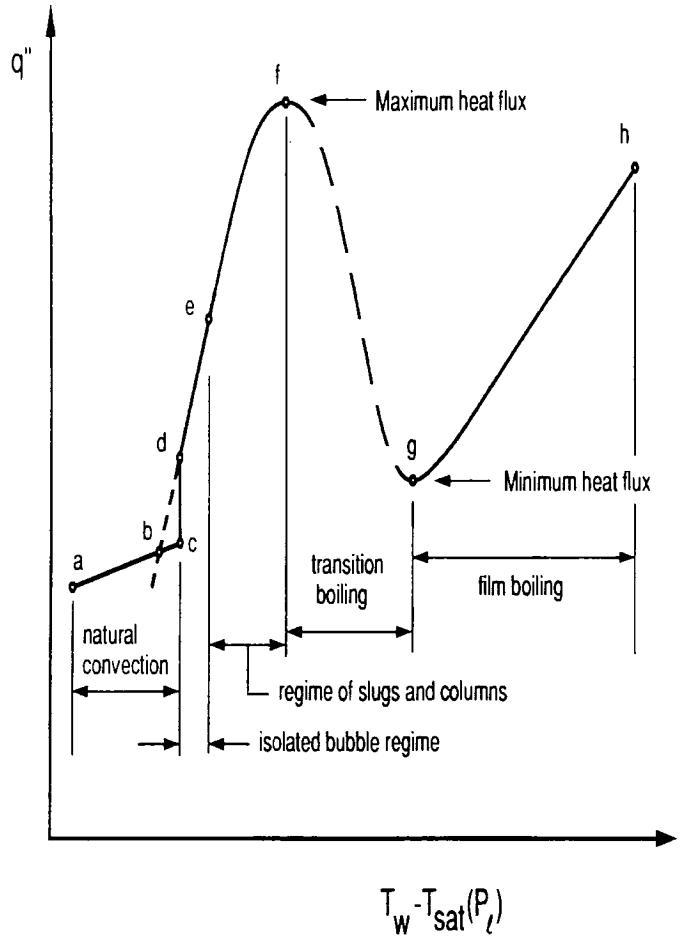

Figure 2.1 Boiling curve for pool and flow boiling

wall superheat ΔT_{sat} at the various axial locations x on the surface versus the local heat flux $\bar{q}$. The numerical values of the temperature difference and $\bar{q}$

are a function of mean velocity, pressure, geometry, thermal boundary conditions and degree of subcooling. The flow boiling curves are generally represented in terms of the local heat transfer coefficient α and quality x. The local heat transfer coefficient is defined by,

$$q''=\alpha\ (T_W-T_{sat}) \qquad \textbf{(2.1)}$$

where T_w is wall temperature and T_{sat} is saturation temperature.

There are four main regimes in boiling: (I) forced and/or natural convection, (II) nucleate boiling, (III) transition boiling, and (IV) film boiling. In forced and/or natural convection case from a to c, the temperature difference T_w-T_{sat} is small. When the temperature difference T_w-T_{sat} is sufficiently large produce regime *c-f* nucleate boiling, three flow patterns are produced.

Firstly, bubbles formed at nucleation sites do not carry into the main stream because the local bulk temperature T_w is still below T_{sat}. When T_w reaches T_{sat} , bubbles appear in the bulk stream. In this situation regime *b-d* occurs. It is sometimes called the *bubbly flow regime*. The bubbles occur throughout the bulk stream and then start to coalesce into slugs of vapor. When T_w is greater than Tsat, more bubbles appear in region from d to f. As a part of d-f, d-e is called the slug flow regime. In this region, the quality is low and the percent volume of the bulk flow occupied by vapor is as large as 50%. As a result, the bulk flow rate increases. In the region e-f, the channel wall is covered by a thin liquid film with vapor. This region is called regime of slugs and columns. At the point which is f

,the heat flux reaches a peak. This peak can be seen from Fig.(2.1) that is called the *departure from nucleate boiling* (DNB). The heat transfer coefficient at the peak is 20 to 50 times as large as the heat transfer coefficient for single-phase flow. This part of the nucleate boiling region is also called the *annular flow regime*.

In region *f-g*, the heat flux decreases dramatically at higher wall superheats. The entire surface becomes blanketed with a vapor film and thermal resistance becomes very large at the surface. This regime is referred to as the *post-dryout regime*.

It was mentioned that in nucleate flow boiling regime, the heat transfer coefficient is very high. Therefore, the wall temperature is close to the saturation temperature. After the peak, the heat transfer coefficients suddenly drops (*f-g*) and again increase (*g-h*). Because of the reduced heat transfer coefficient, the transition boiling and film boiling regions are undesirable in applications such as nuclear reactors and fossil-fuel-fired boilers. On the other hand, transition and film boiling regions sometime occur during accident conditions in nuclear reactors, and a good understanding is needed to manage the thermal conditions.

2.4 Thermodynamics of Binary Mixtures

The equilibrium phase diagram, shown in Fig.(2.2), provides a visual representation of the phase change process in binary mixtures.

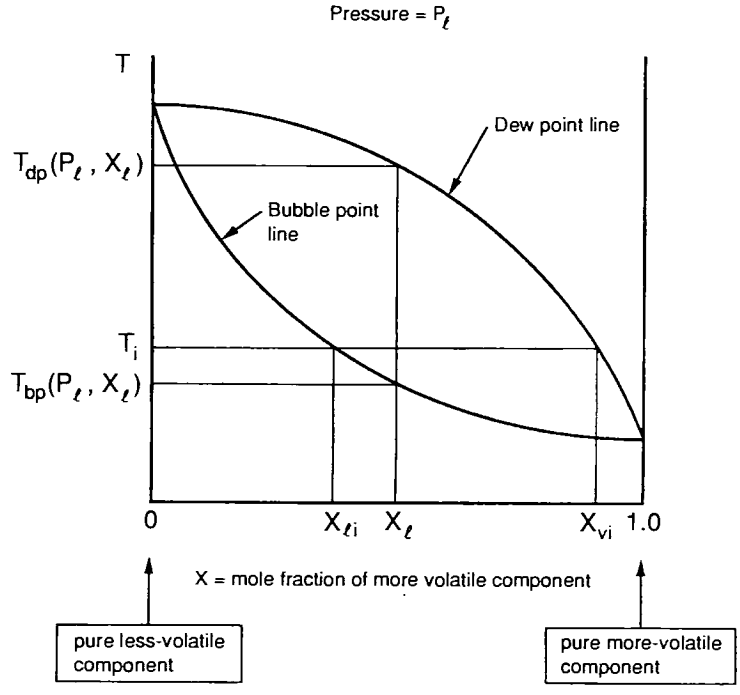

Figure 2.2 Equilibrium Phase Diagram

The equilibrium temperature corresponding to bubble point and dew point are plotted as functions of concentration at a fixed pressure. X_l and X_v are respectively the bulk liquid and vapor concentrations of the more volatile component.

When a binary mixture in vapor phase is cooled at a constant pressure, condensation is first observed. This characteristic of the binary mixture can be

seen from the dew-point curve. Likewise, the bubble-point curve is the locus of points at which vaporization is observed as the binary mixture in liquid phase is heated at a constant pressure.

Using the equilibrium phase diagram, partial pressures, saturation temperatures, mole or mass fractions in equilibrium phases are obtained.

2.5 Nucleate Boiling Heat Transfer

Many investigators obtained the heat transfer coefficients associated with nucleate boiling of binary mixtures by conducting experiments. All experimental studies consist of a series of steady-state boiling tests over the entire liquid range of concentration by keeping the system pressure or system temperature constant. As a result of these experiments, the heat transfer coefficient α_{bl} is calculated by

$$\alpha_{bl} = \frac{q''}{[T_w - T_{bp}(P_l, X_l)]} \tag{2.2}$$

where T_w is the wall temperature and $T_{bp}(P_l, X_l)$ is the bubble-point temperature at the liquid pressure P_l , and the bulk concentration X_l as obtained from the equilibrium phase diagram in Fig.(2.2).

The vapor generated over a nonazeotropic binary liquid mixture is richer in the more volatile component than the bulk liquid. As a nucleating bubble grows,

the liquid at the interface has a lower concentration of the more volatile component as vaporization occurs. The more volatile component diffuses toward the interface, and the less volatile component diffuses away from the interface into the bulk liquid.

The actual temperature at the interface corresponds to the bubble point temperature at the interface concentration of the more volatile component. This, in turn, implies that the temperature at the interface is somewhat higher than the boiling point temperature for the bulk concentration, $T_{bp}(P_l,X_l)$, as seen in Fig. (2.2). The resulting driving temperature difference delivering heat to the interface, T_w-T_s, is less than the temperature difference available corresponding to the bulk saturation conditions. It follows that the amount by which T_w-T_l is less than T_w-$T_{bp}(P_l,X_l)$ increases as the difference between the equilibrium vapor and liquid concentrations $|Y_1$-$X_1|$ increases. Y_1 is mole fraction of more volatile component in liquid phase and X_1 is mole fraction of more volatile component in vapor phase.

At the interface, the vapor and liquid concentrations differ as shown in the phase diagram, Fig.(2.2). The concentration difference in the bulk liquid, $|Y_1$-$X_1|$, is different from the concentration difference at the interface $| Y_{1,s}$-$X_{1,s}|$ due to mass diffusion and/or convection away from the interface. It can be seen from Fig.(2.2) that the difference between the liquid and vapor concentrations at the interface goes to zero at pure liquid component concentrations to a maximum as the concentration varies between the two pure fluid limits.

It can be seen from the above arguments that T_w-T_l is less than T_w-$T_{bp}(P_l, X_l)$. T_w-T_l is zero at the pure component bulk concentrations, and reaches a maximum at some intermediate concentration. Therefore, during nucleate boiling of the mixture at a given pressure and wall temperature, the heat transfer coefficient α_{bl} is determined by eq.(2.2) and the bulk liquid concentration shown in Fig.(2.3). As far as heat transfer is concerned, the mixture would behave like azeotropic mixture (i.e., like a pure fluid with properties that are averages of pure-fluid properties for components in the mixture). For such idealized circumstances, an estimate of the heat transfer coefficient α_{bli} would be a weighted average of the heat transfer coefficients for pure the components:

$$\alpha_{bli}=\alpha_{l0}X_1+\alpha_{h0}(1-X_1) \qquad \textbf{(2.3)}$$

In this relation α_{l0} and α_{h0} are the pure-component heat transfer coefficients at the same pressure and heat flux for the low-boiling –point and high-boiling-point constituents, respectively.

The arguments imply a linear variation of the heat transfer coefficient with concentration, as shown in Fig.(2.3), if mass diffusion is infinitely fast.

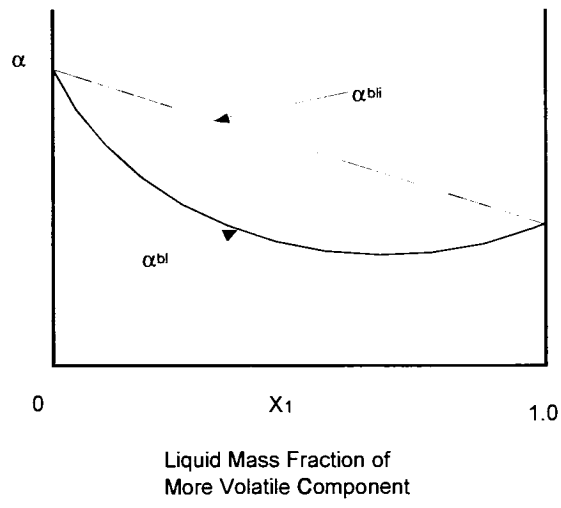

Figure 2.3 Binary Heat Trasfer Coefficient

2.6 Extended Rayleigh Equation

Rayleigh (1917) used a consideration of the increase in bubble pressure resulting from inertial forces imposed on the interface by the surrounding liquid to derive a bubble growth model.

Extended versions of Rayleigh's analysis (1917), which include a more comprehensive approach to the considerations of hydrodynamic effects and momentum transport in a viscous fluid, have been developed by Forster and Zuber (1955), Plesset and Zwick (1954), and Scriven (1959). Plesset and Zwick (1954) showed that for large values of the Jakob number, Ja, the solution to the extended Rayleigh equation is given by the simple form:

$$R(t) = 2\ C_R\sqrt{a_l t} \qquad (2.4)$$

where

$$C_R = \sqrt{\frac{3}{\pi}}Ja \qquad (2.5)$$

This work confirms the validity of the boundary layer assumption made by Bosnjakovic (1930), and the validity of the asymptotic growth solution.

2.7 Van Stralen Model of Mass Diffusion

By considering the analogy between heat and mass diffusion, Van Stralen (1967) established a mass diffusion model that extended the Scriven (1959) and Bruijn (1960) theories for pure-fluid solution into the realm of binary systems. Van Stralen (1967) assumed an asymptotic mode of bubble growth and utilized the fact that the goveming equations for mass diffusion of the more volatile component are analogous to those for heat diffusion. He set forth an equation for bubble growth which is a modification of the Rayleigh equation presented by Plesset-Zwick (eq.(2.4)) as:

$$R(t) = \left(\frac{12}{\pi}\right)^{1/2} Ja_0 (at)^{1/2} \tag{2.6}$$

where Ja_0 is a modified Jakob number for mixtures given by:

$$Ja_0 = \frac{\theta_0}{\left(\frac{\rho_v}{\rho_\ell}\right)\left[\frac{h_{lv}}{c_{p\ell}}\left(\frac{a}{D}\right)^{1/2}\left(\frac{\Delta T_s}{G}\right)\right]} \tag{2.7}$$

D is the mass diffusivity of the more volatile component, and ΔT_s is the difference in the saturation temperatures of the bulk liquid and the liquid in the

bubble interface. G is the vaporized mass diffusion fraction of the bubble and is given by:

$$G = \frac{\left(x_l - x_{l,s}\right)}{\left(y_{l,s} - x_{l,s}\right)} \tag{2.8}$$

G is an expression of the concentration difference across the mass diffusion boundary layer. Here x_l is the liquid mass fraction of the more volatile component in the bulk liquid, $x_{l,s}$ is the liquid mass fraction of the more volatile component at the interface, and $y_{l,s}$ is the vapor mass fraction of the more volatile component at the interface.

Van Stralen showed that for sufficiently small values of the vaporized mass fraction G, the ratio $\left(\frac{\Delta T_s}{G}\right)$ is independent of both G and the wall superheat ΔT_s. Furthermore, he elaborates a graphic method of determining the value of $\left(\frac{\Delta T_s}{G}\right)$ based on the isobaric equilibrium phase diagram for a binary system depicted in Fig.(2.4).

The intersection of the bulk concentration x_l with the boiling point curve establishes the saturation temperature of the bulk liquid T_{sat}. The notion is

utilized that the depletion of the most volatile component in the boundary layer around a bubble

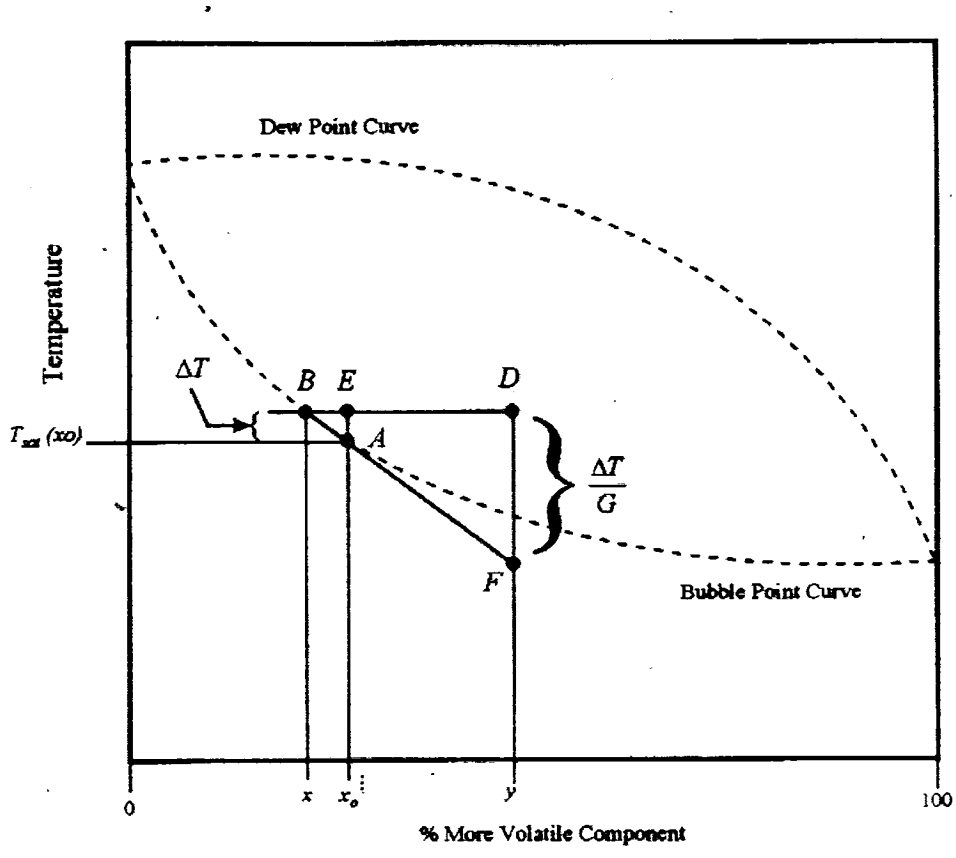

Figure 2.4 Van Stralen's (1967) Equilibrium Phase Diagram

results in an increase in the saturation temperature at the interface by an amount designated ΔT_s. This is graphically represented by the segment AE. Likewise, by an extension of its definition into the graphic above, G is represented by the ratio of the segment lengths BE and BD. Geometric similarity considerations indicate that the ratio $\left(\frac{\Delta T_s}{G}\right)$ is exactly given by the length of

segment DF. Furthermore, based on the assumption of small value of G, that is to say $x_l \sim x_{l,s}$, it should be evident from basic geometry that the segment BAF can be closely approximated by a tangent to the bubble-point curve drawn through point A. This allows an approximation of $\left(\frac{\Delta T_s}{G}\right)$ given only the bulk concentration for the binary system.

The value of $\left(\frac{\Delta T_s}{G}\right)$ is an indication of the relative strength of the mass diffusion mechanism that suppresses bubble growth. Thus, bubble growth rates are minimized at the occurrence of maximum $\left(\frac{\Delta T_s}{G}\right)$ for a particular bulk concentration. This follows directly from the Scriven (1959) solution, and yields a suppression factor S for a binary system:

$$S = \frac{1}{\left[1 + \left\{\frac{1}{c}\left(\frac{a}{D}\right)^{1/2}\left(\frac{T}{G}\right)\right\}\right]} \tag{2.9}$$

2.8 Kandlikar Correlation

One of the latest theoretical correlations which appears in literature is the result of the work of Kandlikar (1997). The correlation was developed by Kandlikar that emphasizes the effects of mixture composition, mass diffusion, liquid concentration at the interface, non-ideality of the mixture, and interface temperature on the heat transfer coefficient of binary mixtures.

Kandlikar utilizes volatility parameter as

$$V_1 = \frac{c_{p.L}}{\Delta h_{LG}} \left[\frac{\kappa}{D_{12}} \right]^{0.5} \frac{dT}{dx_1}(x_1 - y_1) \tag{2.10}$$

Before developing a final expression that is V_1 , Kandlikar establishes the bubble interface concentration as

$$x_{1.s} = x_1 - 0.678 Ja_0 (\kappa / D_{12})^{1/2} (\rho_G - \rho_L)(y_{1,s} - x_1) \tag{2.11}$$

where the Jakob number is

$$Ja_0 = \frac{(T_W - T_{L.sat})}{(\rho_G / \rho_L)\left[(\Delta h_{LG} / c_{p,L}) + (\kappa / D_{12})^{1/2} (\Delta T_s / g)\right]} \tag{2.12}$$

and the liquid-vapor mass fraction ratio, g, is

$$g = \frac{(x_1 - x_{1.S})}{(y_{1.S} - x_{1.S})} \tag{2.13}$$

The following expression is the diffusion coefficient D_{12} that is calculated by the Vignes correlation (1971)

$$D_{12} = (D_{12}^0)^{\bar{x}2} (D_{21}^0)^{\bar{x}1} A_{12} \tag{2.14}$$

where D^0_{12} and D^0_{21} are the self diffusion coefficients determined by Wilke-Change (1955).

$$D_{12}^{0} = 1.1782 \times 10^{-16} \frac{(\phi M_2)^{1/2} T}{\eta_{L,2} V_{m,1}} \qquad (2.15)$$

Similarly D^0_{21} is obtained by interchanging 1 and 2 in eq.(2.15)

A_{12} is the thermodynamic factor to account for the non-ideality of the mixture. Kandlikar et al.(1975) recommended A_{12}=1.0 since it introduces only a small error. ϕ is the association factor for the solvent (2.26 for water, 1.9 for methanol, 1.5 for ethanol, and 1.0 unassociated solvents, Taylor and Krishna, 1993).

The final expressions for the heat transfer coefficient of a binary system obtained by Kandlikar depend on the region of the binary system. These regions are defined by V_1 which is a volatility parameter defined by eq.(2.10). Three regions in the binary mixtures for the heat transfer coefficient are explained in the following paragraphs.

Region I: Near-Azeotropic Region; $V_1 < 0.03$

The near-azeotropic region includes low volatility difference mixtures and azeotropes. In this region, the mixture behaves like an azeotropic which exhibits characteristics similar to pure components.

Region II: Moderate Suppression region, $0.03 \leq V_1 < 0.2$, and Bo>1E-4

In this region, the convective heat transfer becomes dominant and the nucleation is suppressed. Bo represents the boiling number,(=q"/G h_{fg}) which indicates the non-dimensionless heat flux at the wall.

To find the heat transfer coefficient, the following equation was developed by Kandlikar.

$$\alpha_{TP.B}=\alpha_{CBD.B}=1.136\ Co^{-0.9}(1-x)^{0.8}\ \alpha_{LO} + 667.2\ Bo^{0.7}\ (1-x)^{0.8}\ F_{fl}\ \alpha_{LO} \qquad \textbf{(2.16)}$$

F_{fl} is the fluid-surface parameter for the mixture and is given by

$$F_{fl}= x_1F_{fl,1} + x_2F_{fl,2} \qquad \textbf{(2.17)}$$

F_{fl} for water is 1.0 and is currently unknown for ethylene-glycol.

Region III: Severe Suppression Region, (a) $0.03 \leq V_1<0.2$ and Bo<1E-4 , (b) $V_1 \geq 0.2$

$$\alpha_{TP.B}=1.136\ Co^{-0.9}(1-x)^{0.8}\ \alpha_{LO} + 667.2\ Bo^{0.7}\ (1-x)^{0.8}\ F_{fl}\ \alpha_{LO}F_D \qquad \textbf{(2.18)}$$

F_D is diffusion factor for the mixture and is obtained by the following equation

$$F_D=0.678\ [1+(c_{p,l}/\Delta h_{LG})(\kappa/\ D_{12})^{1/2}|\ (y_1-x_1)(dT/dx_1)|]^{-1} \qquad \textbf{(2.19)}$$

where dT/dx_1 is the slope of the bubble point temperature versus x_1 curve.

This region is dominated by the convective effects.

2.9 Summary of Literature

Finlay et al. (1987) conducted experiments with ethylene-glycol/water mixtures covering an operating range appropriate to automotive engine cooling conditions. A copper test section was employed in most of the experiments, although a few tests were conducted in cast-iron sections and aluminum tubing. Their results indicated a need for better predictive methods for correlating the heat transfer data, especially in the high heat-flux region.

Recently there is an increased thrust to shift to propylene-glycol/water mixtures. Propylene-glycol is less toxic than ethylene-glycol and possesses very similar heat transfer characteristics, and therefore appears to be an ideal replacement. Ambrogi et al. (1997) presented a comparison of the two coolants under a wide range of engine operating conditions.

McAssey et al. (1995) conducted experiments to compare the performance of propylene-glycol/water and ethylene-glycol/water mixtures under the range of conditions similar to those existing in normal engine operation. The entire range, from single-phase to saturated boiling was covered. Under these conditions, the performance with the two mixtures was very similar. They also noted a need to develop more reliable predictive methods for these mixtures.

Bhowmick et al. (1996) presented additional data on both fluid mixtures for a wider range of conditions. In their work, the inlet velocity was varied from

approximately 0.4 m/s to 2.5 m/s and the surface heat fluxes reached a maximum of 1.8 MW/m^2. Their results also indicated a general similarity in performance with the two mixtures, and a need for better predictive models in the subcooled flow boiling region.

Bhowmick et al. (1997) presented comparisons between predicted results and experimental data for water and aqueous mixtures of ethylene-glycol and propylene-glycol. Although the Chen (1966) correlation provided the best approximation to the experimental results, the method tended to over-predict the heat transfer coefficient. Using water data obtained as part of the engine test program, a revised Chen correlation was developed. The revision involved a modification to suppression factor in the Chen correlation. With this revised correlation, the authors showed improved predictions for both ethylene-glycol and propylene-glycol mixtures. However, there were no reliable models available in the subcooled flow boiling for mixtures.

McAssey and Kandlikar (1999) examined the applicability of the saturated flow boiling model for mixtures by Kandlikar (1998a and b), and subcooled flow boiling model for pure components by Kandlikar (1998c), to the experimental data of ethylene-glycol/water mixtures obtained by McAssey et al. (1995) and Bhowmick et al. (1996). McAssey and Kandlikar indicated that the entire data set was covered under the convective dominant region, and nucleate boiling dominant region was not observed. Application of the fully developed boiling

correlation from Kandlikar (1998c) showed good agreement with subcooled water data.

The present work is aimed toward establishing the heat transfer characteristics of ethylene-glycol/water mixture over a range of concentration from 0 to 40 percent under flow boiling conditions. This mixture is chosen for binary mixture study as it exhibits significant mass diffusion related suppression effect in boiling. Another reason for using this mixture is its practical utility in automotive engine cooling application.

3. OBJECTIVES OF PRESENT WORK

The present study is aimed at obtaining the experimental data on subcooled flow boiling heat transfer for ethylene glycol mixtures. The data will be obtained at a constant value of local subcooling by setting the bath circulation pump constant temperature for a given mass flow rate to systematically study the variation in heat transfer rate as a function of heat flux and concentration. The theoretical models for fully developed flow boiling and partial boiling will be extended to the binary mixtures.

4. EXPERIMENTAL SETUP AND PROCEDURE

4.1 Experimental setup

A pictoral representation of the experimental setup as shown in Fig.(4.1) was used in this project. The experimental setup was similar to that used by Stumm (1994), Mizo (1995), Howell (1996), Raykoff (1996) and also Spiesman (1997). The test section was designed to simulate flow boiling and also collect data by using the data acquisition equipment.

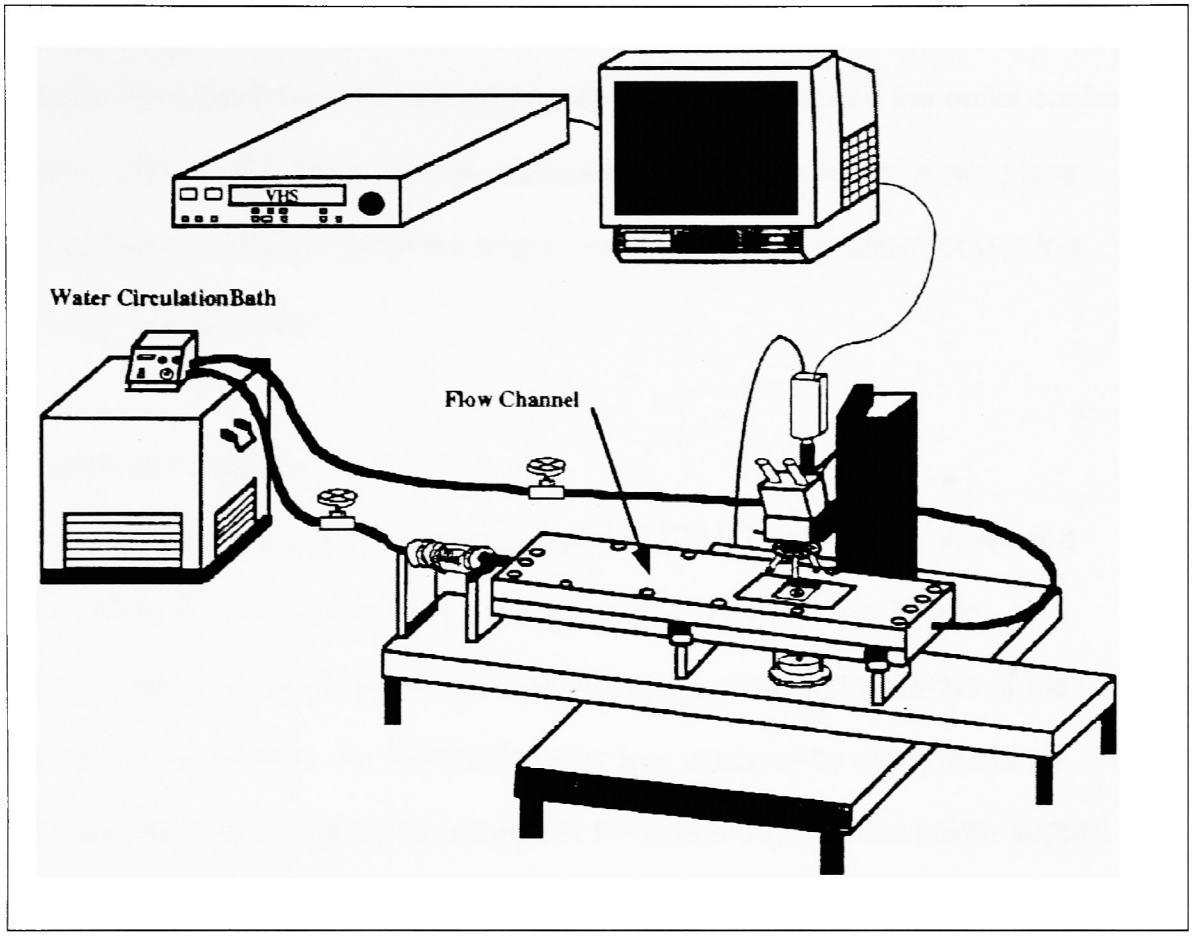

Figure 4.1 Experimental Setup (Adopted from Stumm (1995))

4.1.1 Test Section

The test section consisted of a rectangular channel with a 3mm x 40 mm cross section and 400 mm in length. 2024 –T3 aluminum was used to construct the test section. It also consisted of a constant temperature water bath, flow meter, aluminum heater, microscope, a regular camera, a high-speed camera, power supply, and manometer. It contained an assortment of pipe fittings and connections including valves, elbows, hose clamps, reducing couplings and ½"

I.D high temperature hose. A torlon bushing was used to hold the heater and insulate the heater from the test section. By using the inlet and the outlet control valves atmospheric pressure was maintained in the test section. A two piece polycarbonate window above the heater was put in place to allow for viewing through a microscope.

4.1.2 Heater Element

The heater element was constructed of 6061-T6 aluminum. A set of 4 thermocouples was located along the length of the 9.5mm rod. These thermocouples were set in a radial hole and also located in the center of the cylinder cross section. An electrical heater was wrapped by using the large diameter base of the heater to connect to the power supply. The power supply allowed heater power output in the range 0-200 W. The heater element can be seen in Fig.(4.2), and in detail in Fig.(4.3).

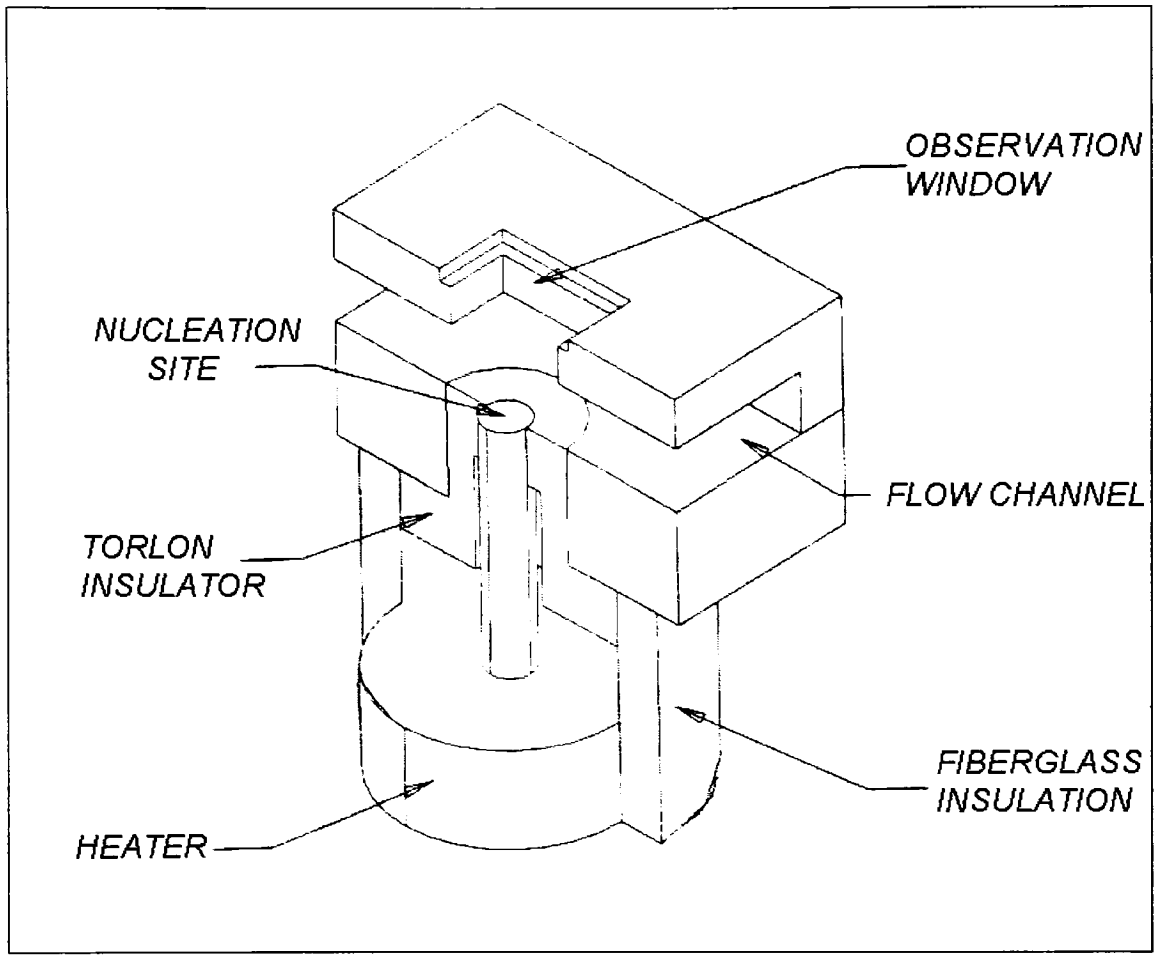

Figure 4.2 Pictorial representation of experimental setup

Adopted from Howell (1996)

4.1.3 Working Fluid

Aqueous solutions of ethylene glycol and pure water were used as the working fluid. Distilled water was used to prevent the formation of deposits on the heater element surface. A volume ratio was used in obtaining the desired mass fraction of each component in the binary mixture based on the specific gravities of each component in the binary mixture. The volume ratio is given in eq.(4.1).

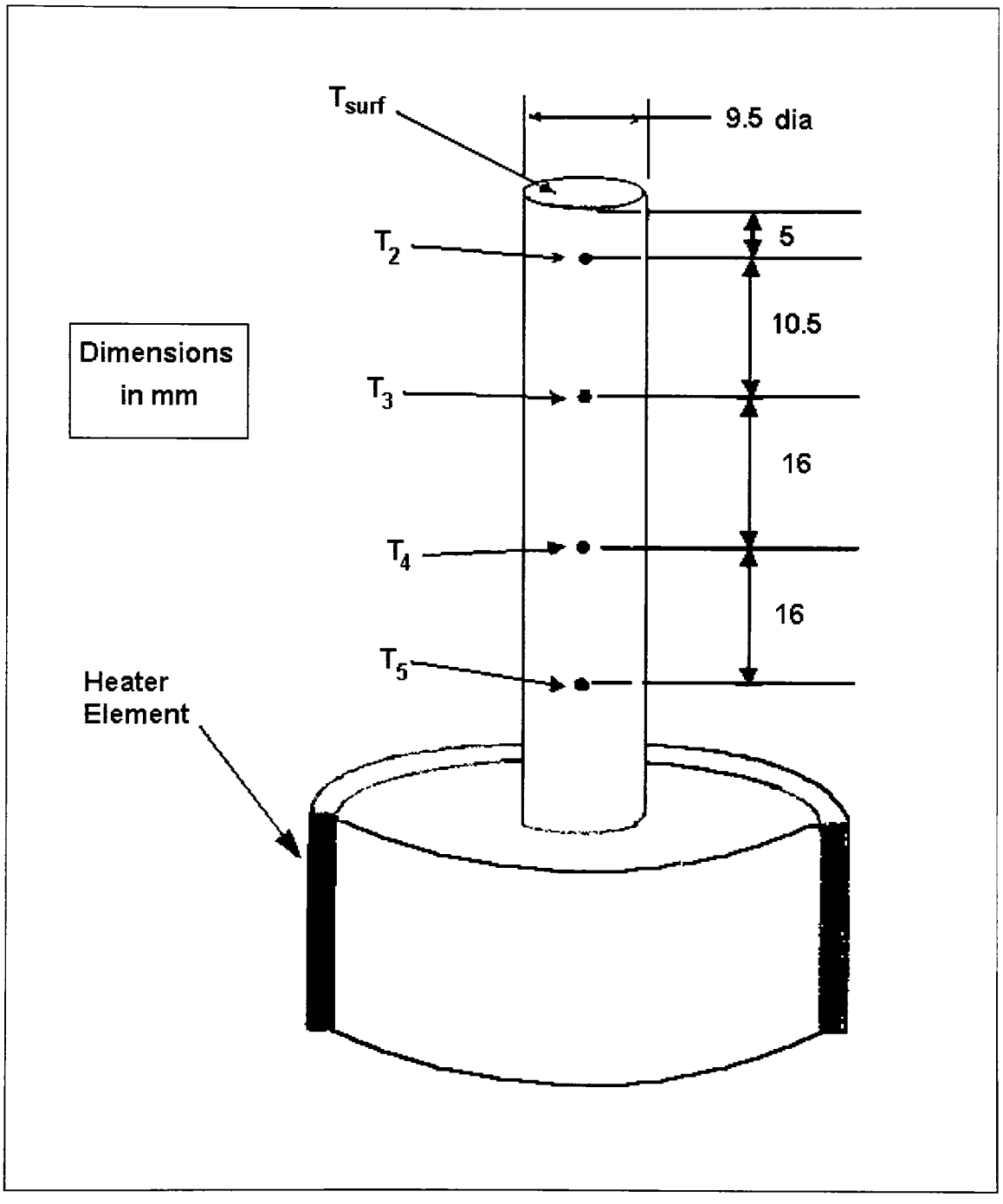

Figure 4.3 Heater element and the location of thermocouples

Adopted from Raykoff (1996)

$$\frac{X * \rho_{EthyleneGlycol}}{(X * \rho_{EthyleneGlycol} + Y * \rho_{Water})} = \%mass_{EthyleneGlycol} \quad \textbf{(4.1)}$$

X is volume fraction of ethylene glycol and Y is volume fraction of water.

4.1.4 Temperature Circulator Pump

The working fluid was circulated and heated by a VWR scientific 1176 constant temperature bath. The circulation pump maintained the water constant temperature and controlled fluid circulation.

4.1.5 Thermocouple Scanner and Thermocouples

Four TT-E-36 type thermocouples were used along the length of the heater to measure the temperature through the heater element. Another thermocouple was located downstream of the flow in the rectangular channel to determine the bulk temperature. Details of the heater and location of the four thermocouples can be seen in Fig.(4.3). The thermocouples were connected to a digital Keithley 740 System Scanning. The temperature readings were observed with a precision of 0.1 C.

4.1.6 Flowmeter

The flow rate was adjusted during the experiment by using an Omega FL-1503A rotameter with a maximum flow of 2.53 GPM. The volume rate of the flow was indicated with a precision of 0.5% of full scale reading.

4.1.7 Fluid Properties

The standard fluid properties were obtained from Alves (1997), and from a Union Carbide (1997) publication for ethylene glycol. The mixture properties were obtained from HYSIM (1996) property routines. The properties of each of the concentrations can be seen in Table 1.

Table 1 Fluid Properties

X_2	Y_2	h_L	h_V	cp_L	λ_L	σ	ρ_L	ρ_V	T_{sat}	Δh_v	μ_L
		J/kg	J/kg	J/kg K	W/m^2	N/m	kg/m^3	kg/m^3	C	J/kg	m^2/s
1	1	-403.119	421.002	3405.68	0.163045	0.032675	968.951	1.64449	197.086	824121	0.000372
0.99	0.961118	-417.255	431.351	3345.89	0.180875	0.036621	977.799	1.561247	186.197	848605.8	4.29E-07
0.98	0.776838	-484.252	480.4002	3301.1	0.197441	0.038678	984.811	1.166716	177.233	964652.1	4.82E-07
0.97	0.693319	-514.616	502.63	3267.8	0.212886	0.040532	990.145	0.987909	169.803	1017246	5.32E-07
0.95	0.535924	-568.38	551.739	3225.48	0.241015	0.041913	998.342	0.829769	158.287	1118099	6.22E-07
0.9	0.299871	-660.71	625.768	3196.55	0.300095	0.043	1008.65	0.680094	140.523	1286478	7.32E-07
0.75	0.089219	-850.675	681.016	3317.91	0.418	0.044292	1013.12	0.603107	118.682	1531691	7.8E-07
0.5	0.024838	-1103.94	687.972	3664.5	0.552371	0.045382	999.291	0.593148	108.842	1791912	6.07E-07
0.25	0.006527	-1346.12	687.0583	4035.59	0.630075	0.046436	974.948	0.59333	102.346	2033173	4.19E-07
0.1	0.002959	-1491.42	686.51	4254.63	0.663878	0.04848	958.873	0.593438	100.797	2177930	3.27E-07
0.05	0.001734	-1532.03	686.4045	4326.43	0.677365	0.051483	953.421	0.593463	100.366	2218438	3E-07
0.03	0.000866	-1560.78	686.3298	4354.96	0.679189	0.052483	951.234	0.593515	100.201	2247107	2.89E-07
0.02	0.000579	-1570.32	686.305	4369.18	0.679189	0.055514	950.14	0.593526	100.119	2256825	2.84E-07
0.01	0.000289	-1580.25	686.284	4383.37	0.68099	0.056541	949.045	0.593533	100.039	2266534	2.79E-07
0	0	-1590.19	686.263	4387.54	0.680684	0.05863	947.95	0.593541	99.9579	2276453	2.79E-07

4.2 Experimental Procedure

4.2.1 Summary of Experimental Procedure

The experiments were performed with pure water and mixtures of ethylene glycol/water in the mass concentration range from 0 to 40 percent ethylene-glycol. For the initial testing runs, distilled water was used as the working fluid in

the system. At the beginning of data collection sessions, the water bath was filled to capacity and the pump and the heater turned on. More water was added to the bath as the level went down due to hoses being filled. First the flow was adjusted approximately 0.129 m/s as a mean velocity. The valve was turned until the meniscus in the pressure tube reached a level approximately equal to the height of the centerline of the flow section and the pump flow rate until the flow meter indicated the proper flow rate. The purpose of doing this was to raise the pressure inside the flow section to atmospheric pressure. The water was continually heated until it reached a temperature of 90 C and allowed to run for approximately three hours to ensure that excess air had been completely eliminated from the water.

When it was seen from the thermocouples reading that the temperature stayed constant that a condition of steady state had been achieved. After that a voltage was applied to a strip heater wrapped around the base of the heater element. A fiberglass cloth was carefully wound around the heater for safety reasons as well as to protect the thermocouple wires from the intense heat that was emitted. The ends of the thermocouple wires were connected to the motherboard of an instrument that translates the thermocouple input into a temperature reading. The four thermocouples used were equally spaced along the length of the heater probe in Fig.(4.3). A fifth thermocouple, downstream of the flow channel after heater element, used to measure the temperature of the water traversing the flow section, revealed the heat losses in the tubing between

the water bath and the flow section. The power supply was increased in five volt increments and was given half an hour to reach steady state before it was determined whether or not nucleation was occurring on the heater surface. At the onset of nucleation, the high-speed camera was used to film this phenomena. Water was run through the system at mean velocities of 0.129 m/s and 0.389 m/s and at temperature of 90, 91, 92, and 93 C.

The next step was to perform the above outlined process utilizing a binary fluid containing ethylene glycol and water. The first binary fluid run through the system contained 1 volume percent glycol and 99 percent water. The mixture was run at mass fraction of 1%, 2%, 3%, 4%, 5%, 7%, 8%, 10%, 12%, 14%, 20%, 25%, 30%, 35% and 40% ethylene glycol as was the case with pure water. The temperature of the water bath was set at the temperature of 90 C, 91 C, 92 C, 93 C, and 95 C and the nucleation was filmed with the high-speed camera as outlined above. The data was logged on a spreadsheet and appears later in this project work. V=0.129 m/s and 0.389 m/s as a mean velocity were again used in data collection. When it was determined that boiling had begun, the high speed camera was again used to film the bubbles leaving the surface of the heater element.

4.2.2 Degasification of Working Fluid

Before gathering the data, binary mixtures were circulated through the test section to remove any dissolved air at a constant bath temperature which is approximately 10 C below the saturation temperature of binary mixture.

4.2.3 Data Acquisition

After the test section reached the steady state condition, the temperatures were measured and recorded every half an hour. At the same time the high speed camera was focused on the bubble activities on the heater surface. When nucleation was observed, the bubble activities were recorded by knowing the magnification of microscope and a frame period of 1ms. Afterwards all the images recorded by using the high speed camera were transferred to a standard videotape. Data numbers were recorded for each session of the high speed camera.

4.2.4 Camera and Microscope

During the experiment a high-speed camera and a regular camera were used to get pictures of the bubbles. A Mitutoyo WF microscope was used to analyze the heater surface. The microscope was attached to the Hitachi KP-C501 solid state camera and was connected to a PC which was loaded with Image –Pro PLUS^{TM} software. 3 various magnification objective lenses of 150X, 250X, and 500X were used in the analysis.

4.3 Experimental Data Reduction

4.3.1 Wall Temperature Reduction

The definition of the heat transfer coefficient used for this work is the ratio of the heat flux into the fluid to the temperature difference between the fluid to the wall temperature at the liquid-wall interface. Because of the difficulty of placing the thermocouple at this actual interface, most heat transfer studies measure the

wall temperature on the outside of the wall and through appropriate analysis determine what the inside of the wall temperature would be. In this work, the surface temperature was estimated by using the same idea which was described above.

4.3.2 Heat transfer coefficient

The experimental heat transfer coefficient is obtained by using equation

$$q''= \alpha\ (T_{sur}-T_{bulk}) \qquad \textbf{(4.3)}$$

From the four thermocouple readings, the surface temperature is obtained .To find the heat flux , the following equation was used

$$q''=k\Delta T/\Delta x \qquad \textbf{(4.4)}$$

This equation holds for the heat flux assuming no heat transfer direction in y,z. Therefore, eq.(4.4) gives the averaged value. By insulating in other direction, it was assumed that the minimal heat losses exist.

4.4 Error Estimation

The surface heat flux, heat transfer coefficient and the surface temperature are calculated by measuring the temperature profile along the length of the circular aluminum heater. The error associated with the measurement of distances between the thermocouple locations is 0.25 mm. The flow rate is measured with a flow meter with an accuracy of ±0.5 percent repeatability of the full-scale value. The flow meter was calibrated with pure water flow. It can be seen from Table 2 that flow velocity measurement is ±0.006 m/s for this

experiment. The thermocouples were calibrated at steam point and ice point, and yield values within 0.1 K at these two conditions. The saturation temperature was calculated from the local pressure measurement and the barometer. The accuracy in the measurement of the saturation temperature is 0.1 K. In order to calculate the standard deviation associated with the measurement precision of various quantities, an experimental run was conducted and readings were taken every three minutes over a period of 2 hours.

The surface heat flux and surface temperature are calculated from the extrapolation of the temperature measurements using one-dimensional conduction model that was described in section 4.3.2.

The total uncertainty U is obtained from its components, bias limit B, and precision limits P, by the following equation.

$$U^2=B^2+P^2 \qquad \textbf{(4.5)}$$

Bias limit is an estimate of the magnitude of the fixed, constant error. The bias limits are determined by calibration tests conducted before and after the experiment or by combining, by root-sum-square method, estimates of elemental bias errors that influence the measurement of the respective variables.

Precision limit is an estimate of the lack of repeatability caused by random errors and unsteadiness. The precision limits can be calculated 2 times of the standard deviation of unsteadiness of a set of observations of T_{wall} and T_{sat}, respectively, measured with apparatus in normal running condition.

Table 2 shows the bias and precision limits obtained from the instrument data, calibration experiments and statistical data obtained with the same setting. The result of the analysis is shown in Fig.(4.4) at V=0.129 m/s. The uncertainty is high near the single-phase region due to smaller temperature difference values. In the region of interest, the uncertainty is in the range of 3-10 percent.

Table 2 Bias Limits and Precision Limits

Bias Limit

Temperature measurement – ±0.1 K
Thermocouple location – ±0.25 mm
Flow velocity measurement - ± 0.006 m/s
Water temperature measurement - ±0.1 K

Precision limits derived from 50 samples

Heater thermocouples - ±0.2 K
Water temperature - ±0.025 K

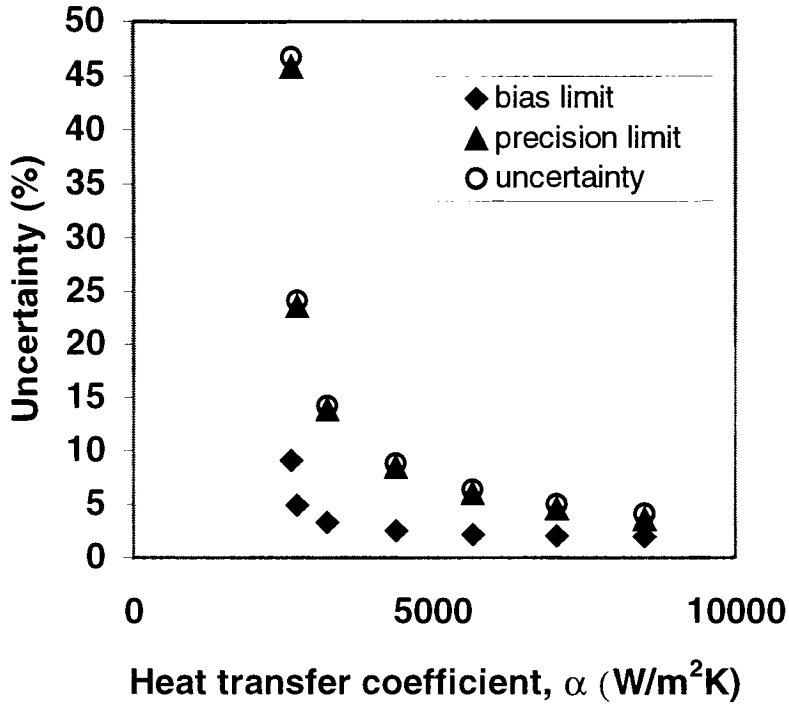

Figure 4.4 Uncertainty associated with the experimental results

5. RESULTS and DISCUSSION

In the experiments, the following quantities were measured: concentration of ethylene glycol , flow rate through the channel, and thermocouple readings along the length of the heater. The thermocouple locations are shown in Fig.(4.3).

The temperature along the heater was used to estimate the heater surface temperature , and the heat flux from the heater to the water flowing in the channel. A regression analysis was performed using a microsoft EXCEL spreadsheet to extrapolate the heater temperatures to predict the heater surface temperature.

From the test section, the heat transfer coefficient can be determined by following the equation of convective heat transfer,

$$q=\alpha A_s(T_{sur}-T_{bulk}) \qquad \textbf{(5.1)}$$

A_s is the wet surface area. The Reynolds numbers are 2446 and 7339 by using eq.(5.2) for the flow rate at 10 % and 30 % of the maximum velocity of 1.33 m^3/s (maximum flow rate of 2.53 GPM) for water. The bulk concentration of binary mixture temperature was 90 C, 91 C, 93 C, 94 C, 95 C, 97 C, 98 C, 99 C. The Reynolds number,

$$Re= \rho v D_h/\mu \qquad \textbf{(5.2)}$$

D_h was calculated by using a hydraulic diameter of 5.58 mm. The hydraulic

$$D_h=4A_c/P \quad (5.3)$$

diameter was calculated using a cross sectional area of 0.00012 m^2 and a wetted perimeter of 0.086 m.

The experiments were performed with a constant temperature of water within +/- 0.1 C. The flow rate was adjusted to yield Reynolds numbers between 2446 and 7339 for the specific water case. All Reynolds number for each concentration of the binary mixtures are listed in Table 3. It can be seen from the table that Reynolds numbers decrease when the binary concentration increases because of viscosity. All the mixture properties were obtained from a property program HYSIM(1996).

The experiments were performed with the heater surface temperature between 5 to 10 C below the saturation temperature . The heat transfer performance for different concentration of binary mixture is studied . It was observed that the heat transfer stays constant in the single phase region and at certain superheat the heat transfer increased rapidly . The heat transfer in the single-phase region is determined by

$$\alpha=\alpha_{convective} \quad (5.4)$$

In this region heat is transferred by convection. When the nucleation takes place,

$$\alpha=\alpha_{convection}+\alpha_{nucleation} \quad (5.5)$$

It was observed from the experiments that nucleation takes place somewhere between 5 C and 12 C superheated for binary mixtures. A rapid increase in heat

transfer coefficient α can be seen in Fig.(5.3) and (5.5).

Reynolds Numbers		
Concentration	**%10 flow rate**	**30 % flow rate**
Pure water	2446	7339
1%	2448	7336
2%	2412	7236
3%	2375	7124
4%	2330	6991
5%	2296	6887
6%	2262	6786
7%	2222	6667
8%	2191	6574
10%	2141	6422
11%	2090	6271
12%	2057	6171
14%	1994	5981
20%	1822	5467
25%	1702	5107
30%	1577	4730
35%	1399	4197
40%	1278	3833

Table 3 Reynolds numbers of ethylene-glycol / water concentration

5.1.Effect of Concentration on Heat Transfer

5.1.1 Volatility Parameter

An analysis of the heat transfer in the flow boiling of binary mixtures utilizes the volatility parameter, V_1 in eq.(2.10), as a measure of the mass diffusion strength. Kandlikar (1998c) utilizes this parameter in the flow boiling of binary mixtures. It is shown that for $V< 0.03$, the mixture effects were negligible. Therefore, the binary mixtures behaved like a pure component without mass diffusion effects.

Fig.(5.1) shows variation of the volatility parameter with concentration. It can be seen from the figure that at low concentrations of ethylene-glycol, up to 10 percent, the value of V_1 is less that 0.005. In this range, the binary effects would be negligible.

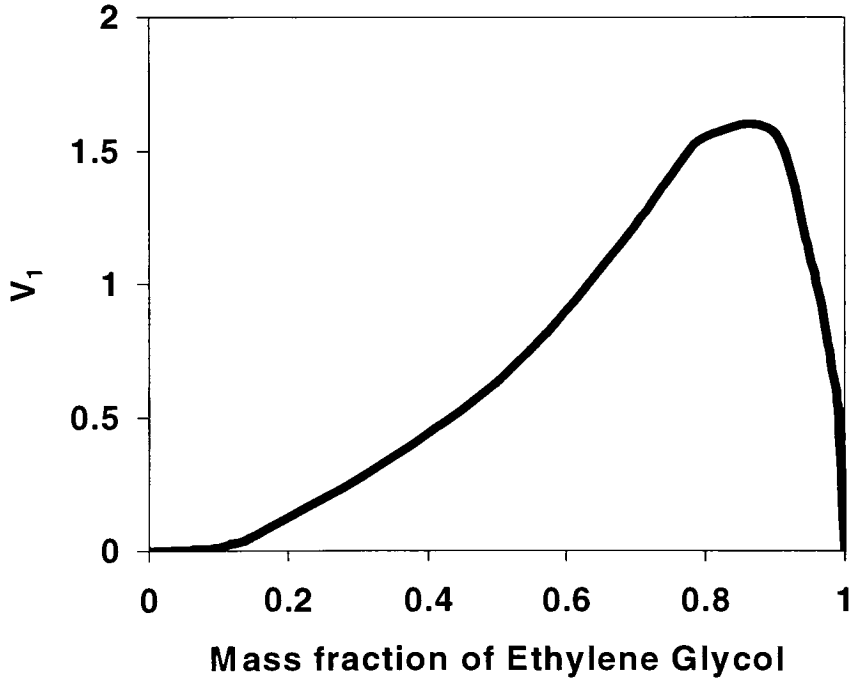

Figure 5.1 Variation of the Volatility Parameter (in the Kandlikar (1998c) Correlation scheme for binary Mixtures) for Ethylene Glycol Mixture at atmospheric pressure

5.2 Experimental Data: Heat Transfer Coefficient

The goal of experimental investigation was to obtain the experimental values of heat transfer coefficient as a function of wall superheat for different concentrations of ethylene-glycol/water mixtures. This required the verification of the validity of the experimental results.

Experimental results are obtained for pure water and, ethylene glycol/ water mixtures with ethylene glycol mass fractions of 1%, 2%, 3%, 4%, 5%, 6%, 7%, 8%, 10%, 11%, 12%, 14%, 20%, 25%, 30%, 35% and 40%. Two flow velocities of 0.129 m/s and 0.387 m/s are employed. The inlet subcooling ranged from 5-10 K. The maximum wall superheat was 25 K.

Fig.(5.2) shows a comprehensive plot of heat flux versus wall superheat for a mean flow velocity of 0.129 m/s. To reduce overcrowding the plot, results for water and only seven other concentrations are shown. As the properties change, the flow Reynolds number changes for each concentration. Individual values of Reynolds number and inlet subcooling for the respective runs are also shown in Fig.(5.2). All properties are calculated at the respective saturation temperatures of the mixture.

As seen from Fig.(5.2), as the concentration of ethylene glycol increases, the heat transfer performance deteriorates (larger superheat is needed for the same heat flux). Addition of just 1% ethylene glycol resulted in significant reduction in heat transfer compared to pure water. As the concentration of ethylene glycol increased, the curves systematically shifted to the right corresponding to higher wall superheat values.

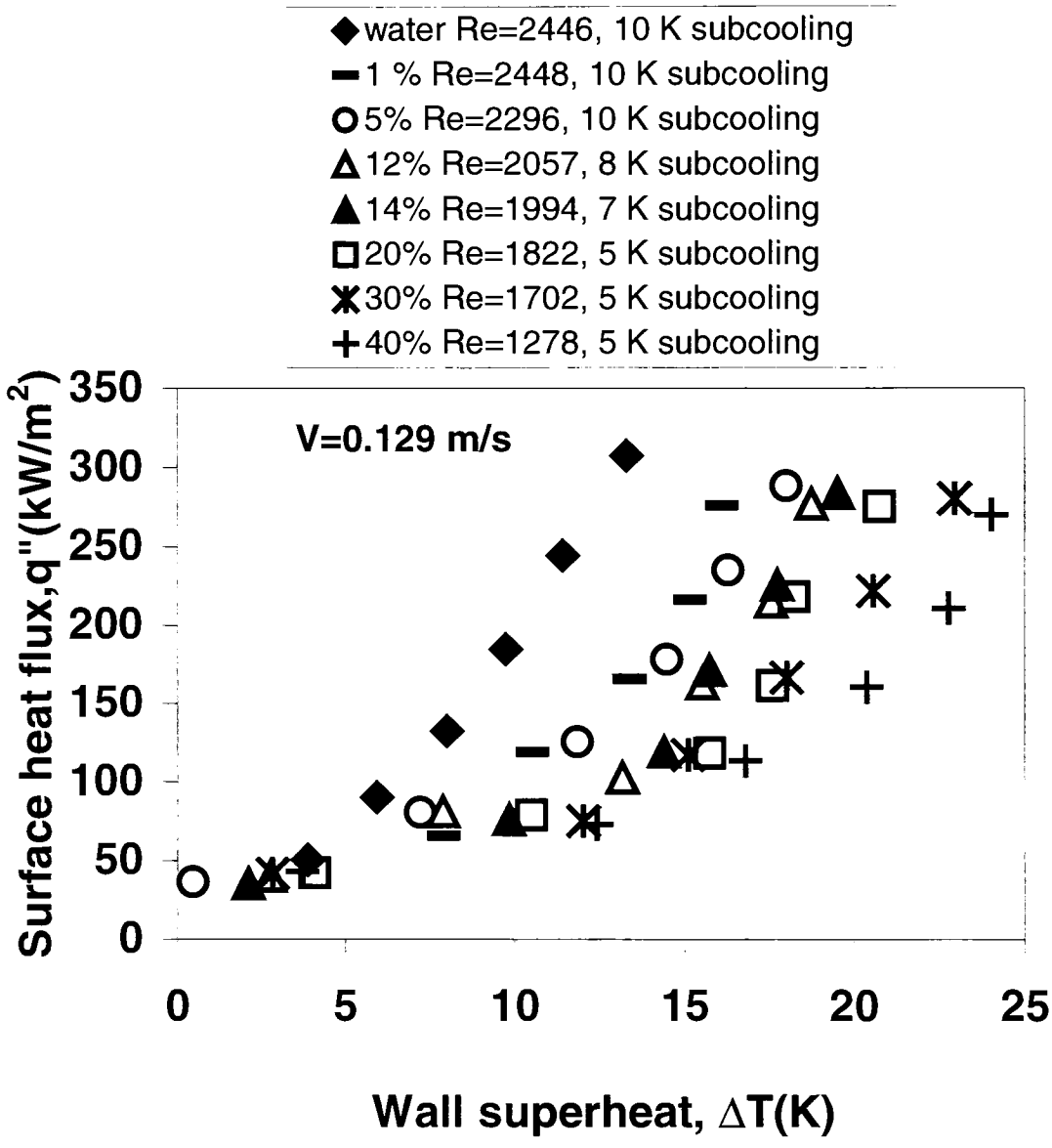

Figure 5.2 Surface heat flux versus wall superheat for flow boiling of water/ethylene glycol mixtures at V=0.129 m/s, (channel hydraulic diameter 5.58 mm, mass fraction of ethylene glycol)

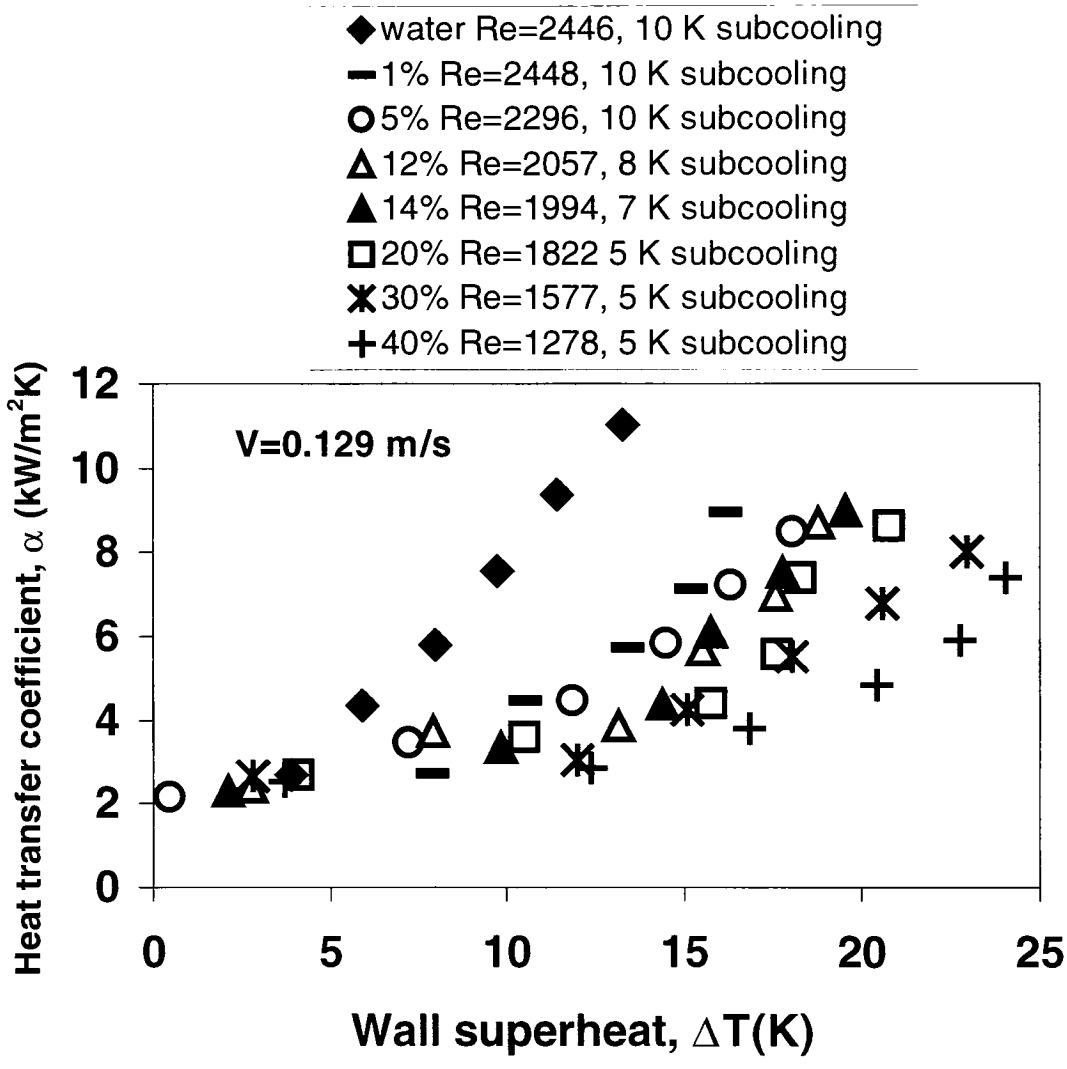

Figure 5.3 Heat transfer coefficient versus wall superheat for flow boiling of water/ethylene glycol mixtures at V=0.129 m/s, (channel hydraulic diameter 5.58 mm, mass fraction of ethylene glycol)

The results from Fig.(5.2) are redrawn with heat transfer coefficient versus wall superheat axes in Fig.(5.3). At lower heat fluxes, the heat transfer coefficient corresponds to the single-phase value before the onset of nucleate boiling. As concentration of ethylene glycol increases, the heat transfer coefficient value at a given wall superheat decreases. It should be noted that the saturation temperature for each concentration is different, and has been accounted for in the calculation of the wall superheat and liquid subcooling.

Similar results are obtained for a higher velocity of 0.387 m/s as shown in Fig.(5.4) and (5.5). Similar deterioration in heat transfer is observed as the concentration of ethylene glycol increases. The rate of increase in heat transfer rate and heat transfer coefficient values with wall superheat becomes lower as the concentration increases. This indicates the increased contribution from the forced convection effects at higher concentrations. Another point to note is that the single-phase heat transfer coefficient values seen at low values of wall superheat are scattered over a range for different concentrations. The reason for this is that the Reynolds number for the same velocity becomes smaller as the concentration increases. Also, the uncertainty is higher in this region as seen Fig.(4.4). The data sets for the low velocity runs are in the laminar and transition regions.

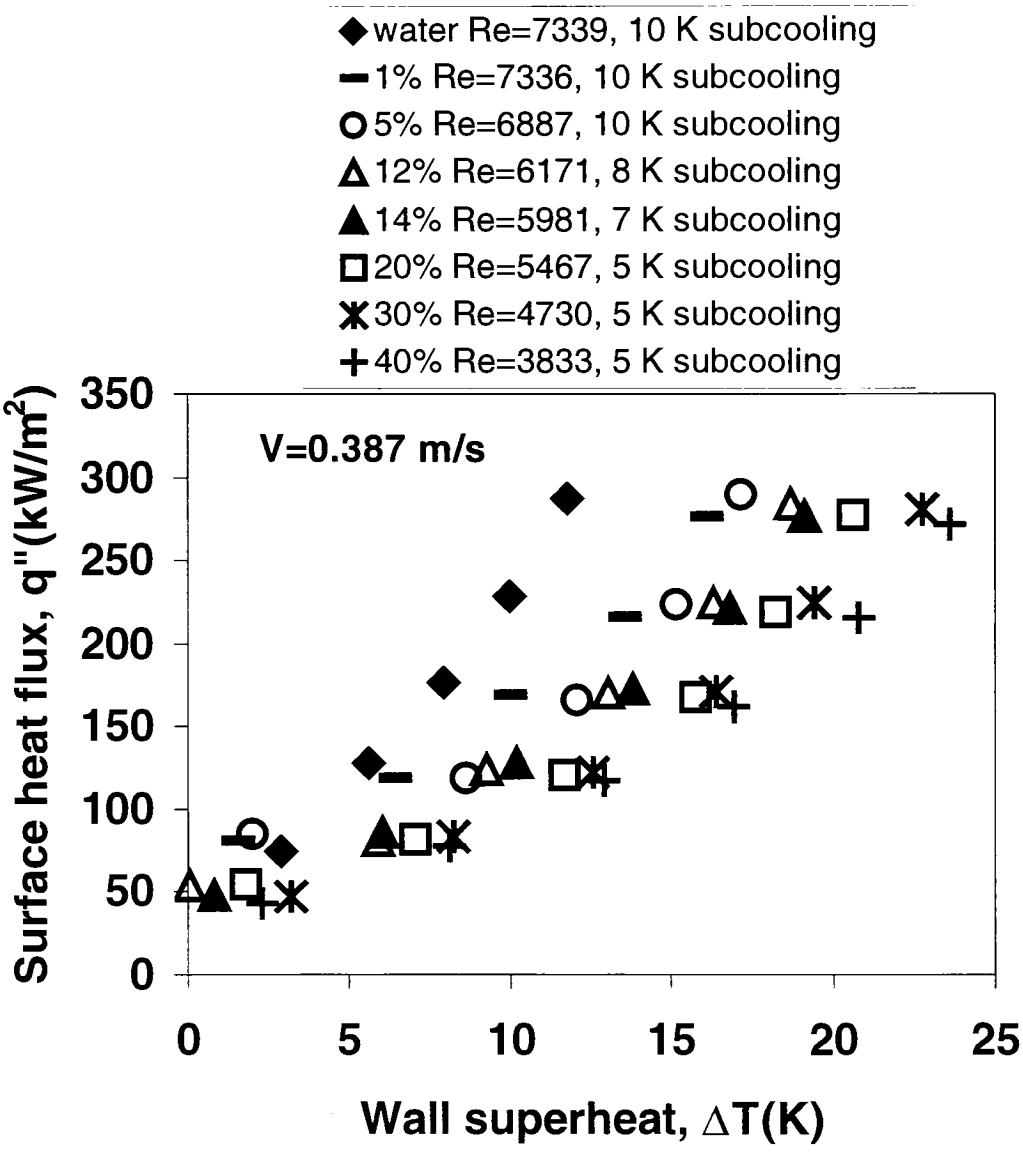

Figure 5.4 Surface heat flux versus wall superheat for flow boiling of water/ethylene glycol mixtures at V=0.387 m/s, (channel hydraulic diameter 5.58 mm, mass fraction of ethylene glycol)

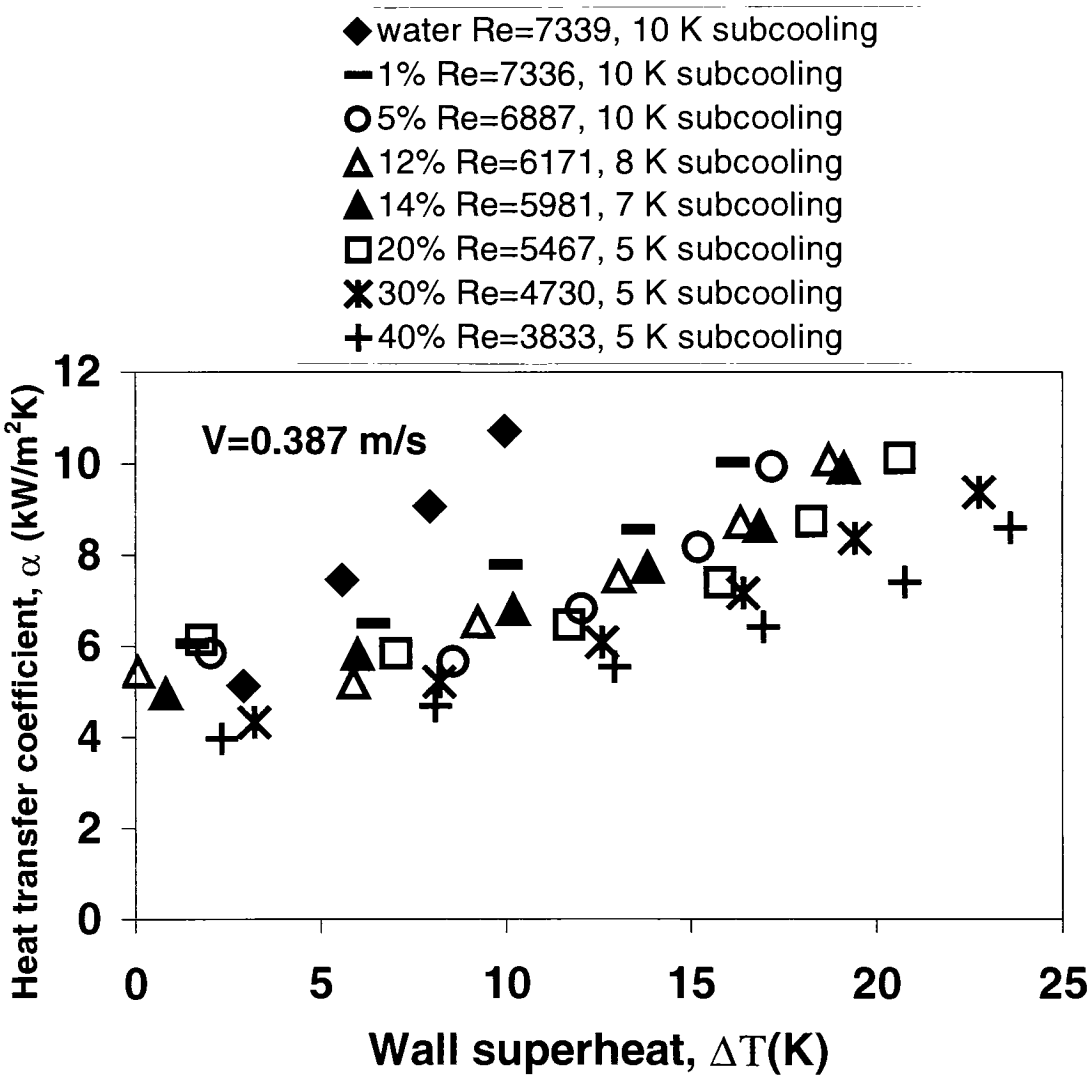

Figure 5.5 Heat transfer coefficient versus wall superheat for flow boiling of water/ethylene glycol mixtures at V=0.387 m/s, (channel hydraulic diameter 5.58 mm, mass fraction of ethylene glycol)

5.2.1 Experimental Heat Transfer Coefficient for Pure Fluids

Heat transfer coefficient for the pure fluid is discussed as the base case for comparison with binary mixture data. One data condition shown in the fluid chart of Fig.(5.3) is 90 C bulk temperature for V=0.129 m/s at Reynolds number of 2446 and the other data condition shown in the fluid chart of Fig.(5.5) is 90 C bulk temperature for V=0.389 m/s at Reynolds number of 7339 by taking the vertical axis intercept at low values of superheat, the single phase heat transfer coefficient can be determined. It can be seen form the graph that heat transfer coefficients are 2676 W/m^2 K for the low flow rate and 5144 W/m^2 K for the high flow rate data points. Single-phase heat transfer coefficient is expected to increase with increasing Reynolds number. It can also be seen from Fig.(5.3) and (5.5) that there is a point from where the heat transfer coefficient starts to increase with an increase in wall superheat. This point is known the onset of nucleate boiling (ONB point). A sharp increase is also observed in the number of active nucleating cavities.

The Reynolds number has a strong impact on the overall heat transfer coefficient at superheat values below the ONB point because single-phase mechanism is dominant in this region.

5.2.2 Experimental Heat Transfer coefficient for Binary Mixtures

Fig.(5.2) and (5.4) show heat flux versus concentration of ethylene glycol. By making a comparison between the binary mixtures and pure fluid data, suppression of the heat transfer coefficient in the binary mixtures is obvious. The suppression is stronger when the concentration of binary system increases from pure water to 40% ethylene glycol. Single-phase values are lower for the binary fluid cases which is given by the variation in Table 1. In this table, pure water solutions have higher conductivity than ethylene glycol. From Fig.(5.3) and (5.5). it can be seen that more significant is the suppression of the sharp rise in heat transfer coefficient at the ONB points. Nucleate boiling is suppressed especially in the higher concentrations of ethylene glycol mixture.

In considering the behavior of the heat transfer coefficient over the entire range of concentrations, it is obvious that there is a relationship between the heat transfer coefficient and concentration of ethylene glycol. As the concentration of ethylene glycol increases, the heater surface superheat increases. It can be attributed to the fact that a larger number of nucleation sites become active as the heat flux increases.

5.3 Hysteresis

Binary mixtures yield lower heat transfer coefficients than pure water for the same wall superheat condition. Comparing the tests with increasing heat flux with those obtained with a decreasing heat flux, it was observed that there is a significant difference between the two near the onset of nucleate boiling.

To see the effect hysteresis, experiments were conducted for both decreasing and increasing heat fluxes. The results presented here correspond to heater performance after cycles of increasing and decreasing heat fluxes. Fig.(5.6), (5.7), (5.8) and (5.9) show such plots for pure water and 6% concentrations of ethylene glycol, and flow velocities of 0.129 m/s and 0.387 m/s. The hysteresis effects were most significant at the start-up. For low velocity runs, a slight hysteresis effect (5 percent difference in heat flux) was observed for mixtures in the region 0-10 K wall superheat. This effect was very small for high velocity (0.387 m/s) runs.

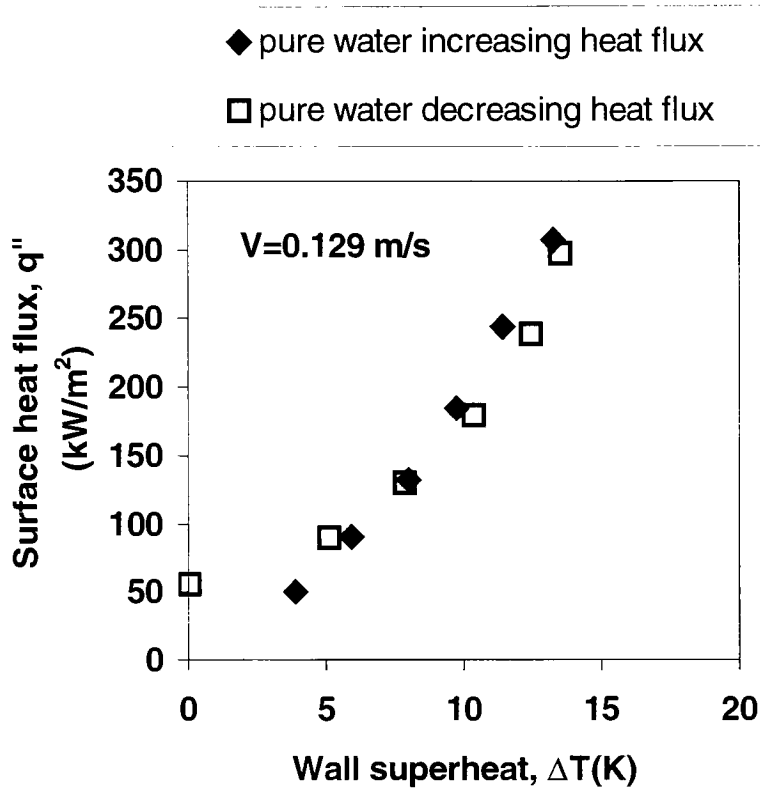

Figure 5.6 Effect of hysteresis on flow boiling heat transfer for pure water at V=0.129 m/s, (channel hydraulic diameter 5.58 mm)

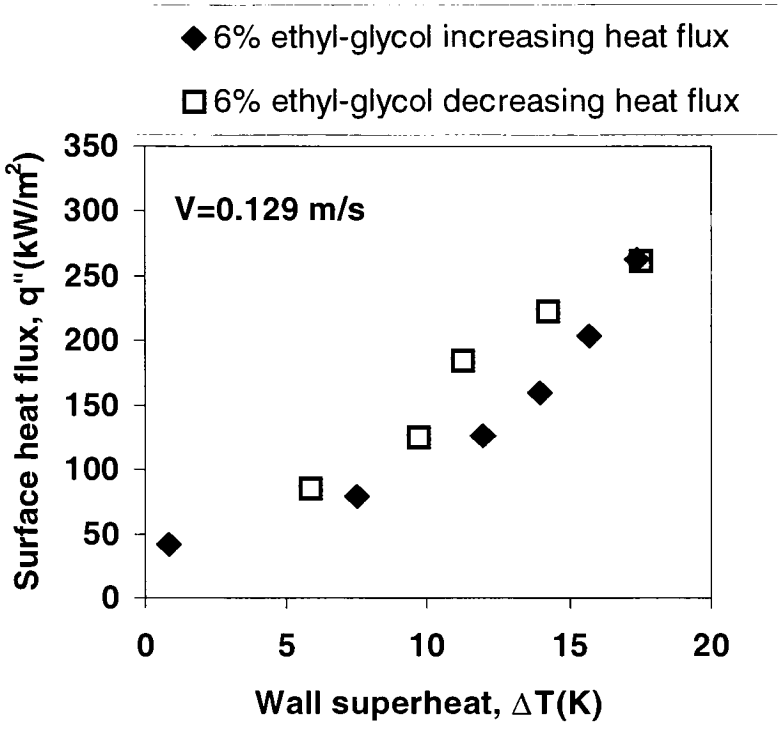

Figure 5.7 Effect of hysteresis on flow boiling heat transfer for 6% ethylene-glycol/water mixture at V=0.129 m/s, (channel hydraulic diameter 5.58 mm)

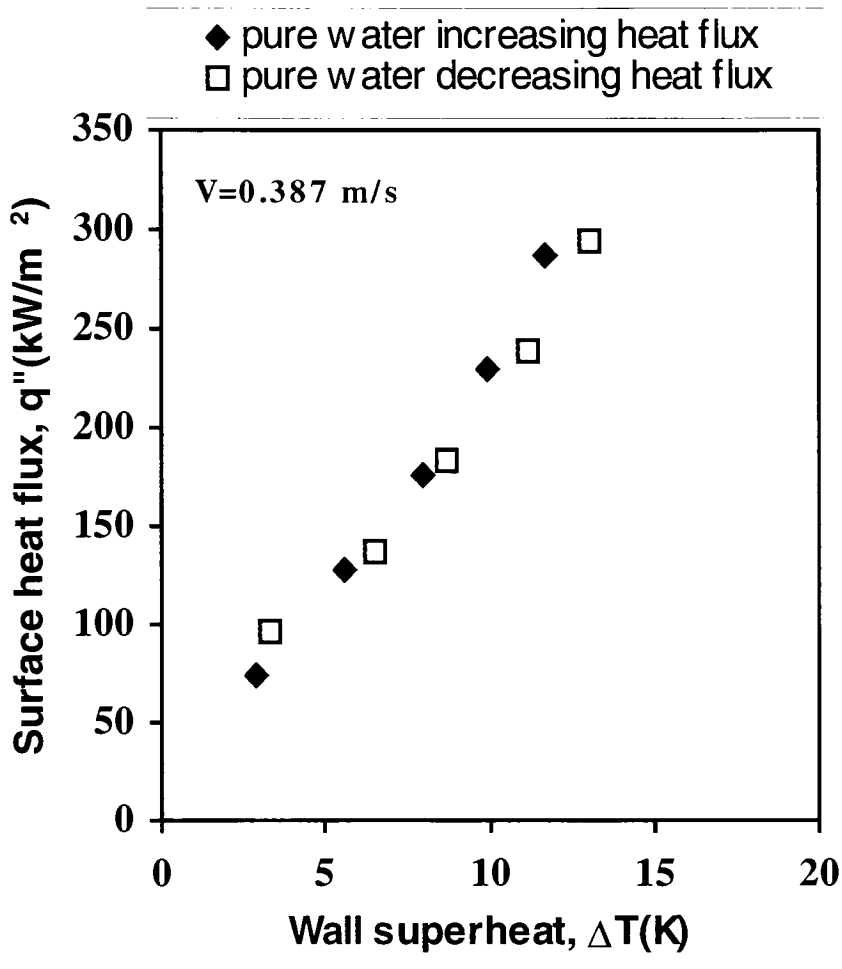

Figure 5.8 Effect of hysteresis on flow boiling heat transfer for pure water at V=0.387 m/s, (channel hydraulic diameter 5.58 mm)

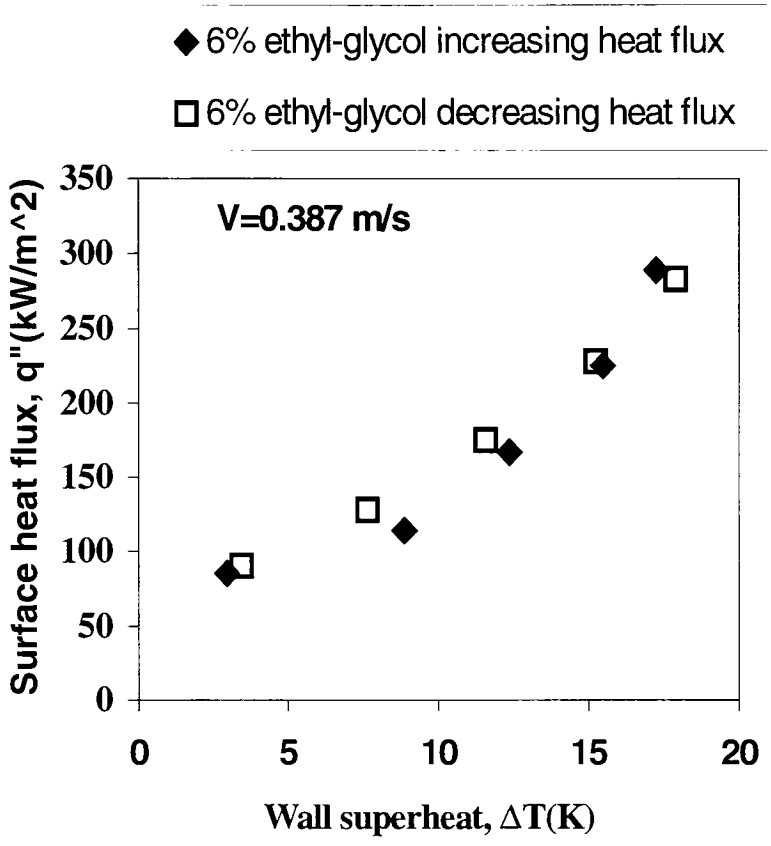

Figure 5.9 Effect of hysteresis on flow boiling heat transfer for 6% ethylene-glycol/water mixture at V=0.387 m/s, (channel hydraulic diameter 5.58 mm)

Fig. (5.10) is an example of hysteresis that was found experimentally Marto et.al (1968). In the present work, the hysteresis effect is very small as seen from Fig.(5.6)-(5.9)

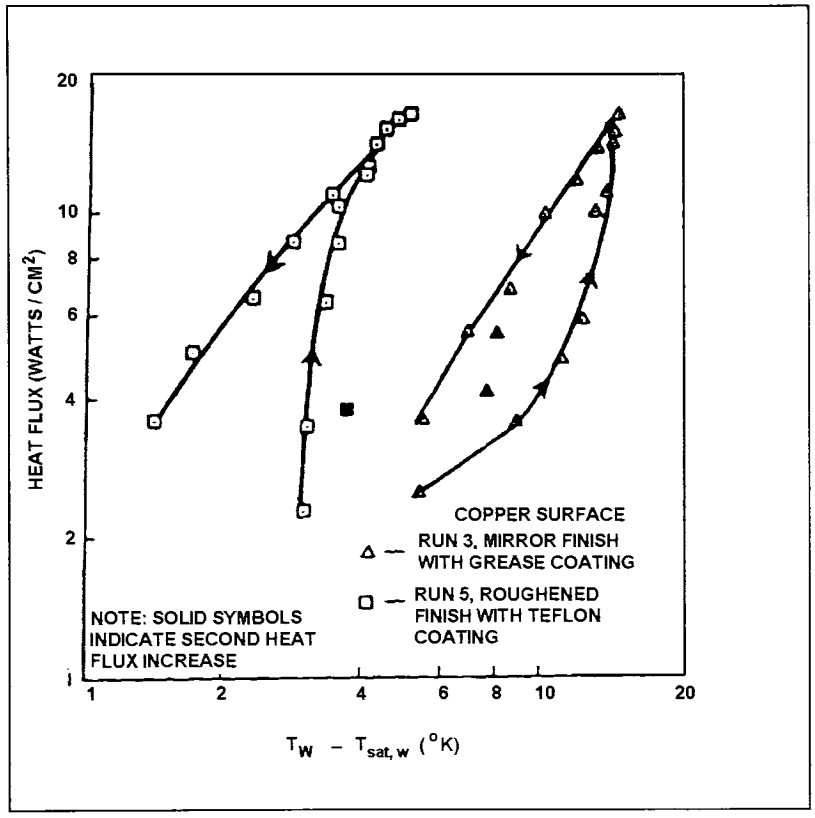

Figure 5.10 Effects of hysteresis

Adopted from Marto et.al (1968)

5.4 Comparison with Fully Developed Flow Boiling Correlation and Extension to Binary Mixtures

Heat transfer in the subcooled boiling region is classified in partial boiling and fully developed boiling regions. Kandlikar (1998a) presented a comprehensive methodology to predict heat transfer in these regions for pure liquids. One of the major aspect of their methodology is the prediction of the heat transfer coefficent in the fully developed boiling region using the Kandlikar (1990) correlation. Heat transfer in the fully developed boiling region for pure fluid is given by:

$$\begin{aligned} q'' &= \alpha_{TP}(T_W - T_f) \\ &= \alpha^*(T_W - T_{sat}) \\ &= 1058 Bo^{0.7} F_{fl} \alpha_{lo}(T_W - T_{sat}) \end{aligned} \qquad (5.6)$$

α_{TP} in eq. (5.6) is based on $(T_w - T_f)$, where T_f is the bulk liquid temperature and α^* is based on $(T_W - T_{sat})$. According to eq.(5.6), there is no effect of subcooling on heat transfer in the fully developed boiling region. F_{fl} is a fluid-dependent factor in the Kandlikar (1990) correlation. F_{fl} for mixtures is obtained as a mass fraction-averaged value for the two pure constituents. Since the value of F_{fl} is not reported for ethylene-glycol, it is used as 1 (same as water) in the present work.

Kandlikar (1998c) presented a methodology for predicting heat transfer in saturated flow boiling of binary mixtures. He identified three regions to describe

the level of binary effects. (a) In the near-azeotropic region, the mass transfer effects were negligible, and the heat transfer was given by the pure component equation. (b) In the moderate suppression region, nucleation was suppressed to some extent and the heat transfer was described by the equation applicable in the convective boiling dominant region. (c) In the severe suppression region, the heat transfer was further reduced and a factor F_D was introduced in the nucleate boiling term to represent the mass diffusion effects.

Extending the above models to binary mixtures, the heat transfer in the fully developed boiling region can also be classified depending on the level of suppression. In the near-azeotropic region, eq. (5.6) is expected to apply. In moderate suppression region, the nucleate boiling term in the equation applicable to the convective boiling dominant region is used. It is given by:

$$q''=667.2\ Bo^{0.7}F_{fl}\alpha_{lo}(T_W-T_{sat}) \qquad \textbf{(5.7)}$$

In the severe suppression region, the heat transfer is further reduced by a factor F_D .The final expression for fully developed nucleate boiling is given by

$$q''=667.2\ Bo^{0.7}F_{fl}\alpha_{lo}(T_W-T_{sat})\ F_D \qquad \textbf{(5.8)}$$

The diffusion induced suppression factor F_D is given by:

$$F_D=0.678\ [1+(c_{p,l}/\Delta h_{LG})(\kappa/\ D_{12})^{1/2}|\ (y_1-x_1)(dT/dx_1)|]^{-1} \qquad \textbf{(5.9)}$$

A volatility parameter V_1 was used to describe the level of suppression. It is given by eq.(2.10).

It can be seen from eq.(2.10) that dT/dx_1 is the slope of the temperature versus liquid concentration curve, and y_1 is the equilibrium vapor concentration. Fig.(5.10) shows the variation of V_1 with concentration for ethylene glycol mixture. According to Kandlikar (1998c), for $V_1 < 0.03$, the mixture can be treated as a pure component; moderate suppression region covers $0.03 < V_1 < 0.2$ (with further dependence on Boiling number), and severe suppression region extends beyond $V_1 > 0.2$.

Applying the criteria described above, the mixture can be treated as a pure component below a concentration of 0.15, and eq.(5.6) applies in the fully developed boiling region. For concentrations of 0.15 and 0.4, the mixture falls under moderate suppression region, and eq.(5.7) applies. The experimental data obtained in this investigation does not cover the severe suppression region.

In a separate study, McAssey and Kandlikar (1999) compared their ethylene glycol/water mixture data obtained from automotive engine cooling application with eq. (5.7) and found good agreement to within ±30 percent. They also indicated that the prediction accuracy will improve with the incorporation of accurate F_{fl} for ethylene glycol, inclusion of the factor F_D, and the extension of the Kandlikar's (1998a) partial boiling methodology to mixtures.

It should be noted that there is some uncertainty involved in the present comparison due to the non-availability of the fluid-dependent factor for ethylene glycol). Experimental data for pure ethylene glycol could not be obtained (to evaluate F_{fl}) in the present work due to its high boiling point.

Fig.(5.11) shows the results for pure water using eq. (5.6) from the Kandlikar's (1998a) FDB correlation. As the wall superheat increases, the heat transfer approaches the fully developed boiling for which eq. (5.6) is applicable.(Note that eq.(5.6) does not apply in the partial boiling region at lower values of wall superheat). It is seen that the data merges into the FDB correlation predictions for both flow velocities, and the agreement is very good. This also indicates that the present experimental setup using a rectangular flow channel and a circular spot heater yields similar results to the circular geometry in flow boiling application.

Fig.(5.12) shows the experimental data for 5% ethylene glycol solution at two flow rates. Also, shown in the figure are the predictions from eqs. (5.6) and (5.7). At this concentration, the value of V_1 from Fig. (5.1) is seen to be close to zero, and the diffusion effects are expected to be very small. The data reflects this expected behavior as it lies between the two prediction curves. However, as the concentration increases to 11%, the results shown in Figure 5.13 indicate a very good agreement between the data and predictions from eq. (5.7).

Fig.(5.14) and (5.15) show the results for 30% and 40% concentration respectively. Here the diffusion effects are expected to be somewhat higher, and eq.(5.7) should be applicable. Further effects of mass diffusion are seen in Fig.(5.15) for 40% solution, and eq.(5.8) needs to be considered at higher concentrations. Final conclusions must wait until F_{fl} for ethylene glycol is determined first from experiments.

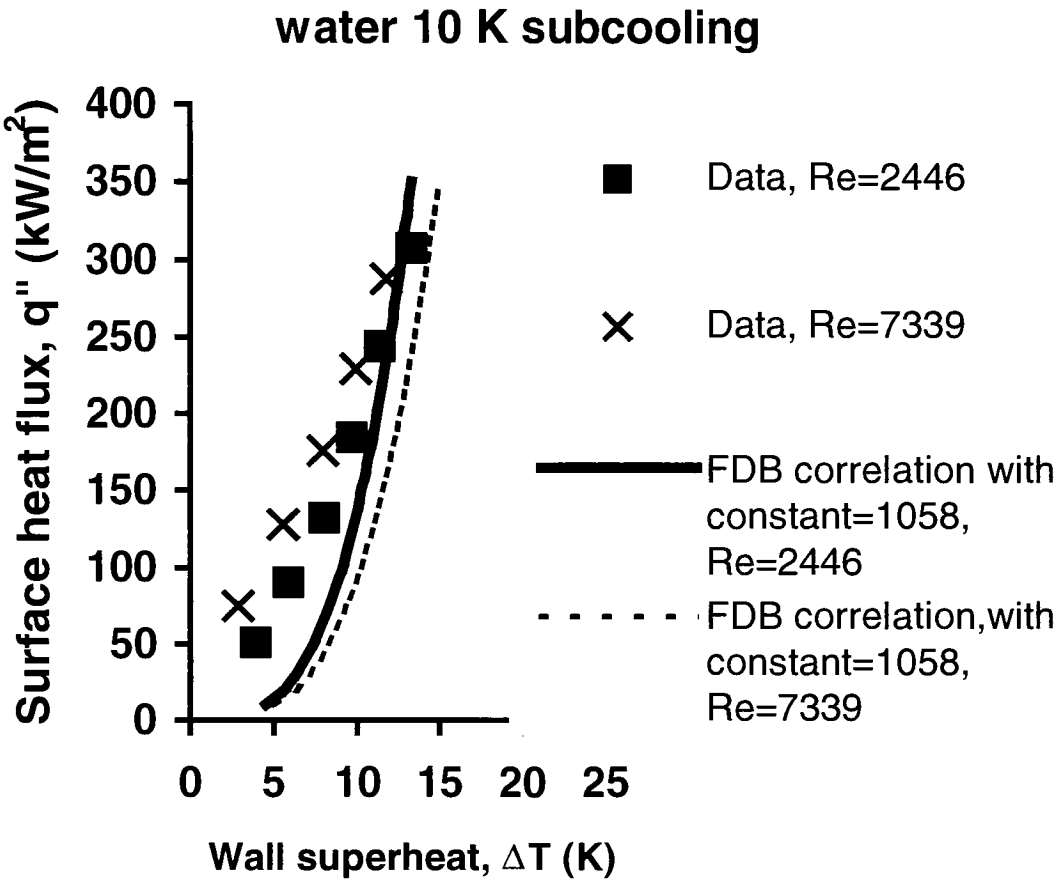

Figure 5.11 Comparison of the Present Data with the FDB correlation for Pure Water by Kandlikar (1998a), eq. (5.6), at two flow velocities

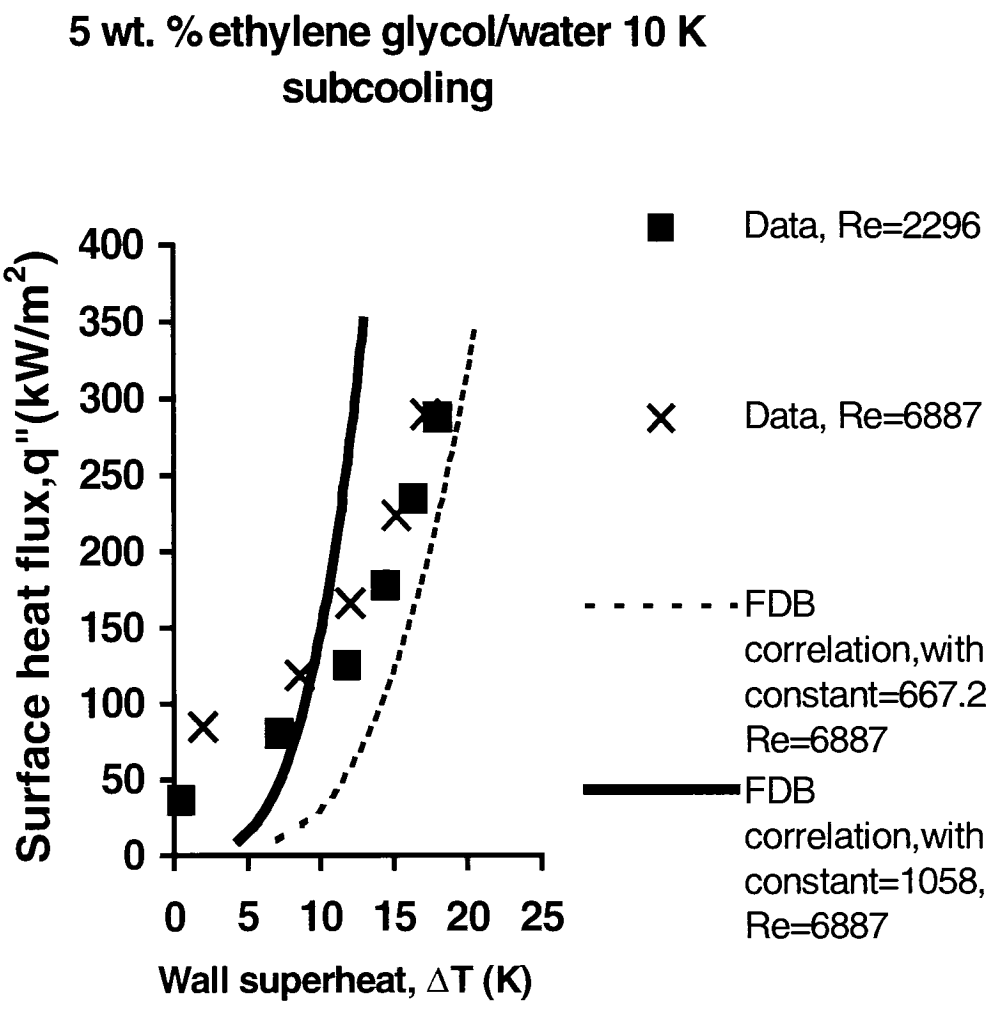

Figure 5.12 Comparison of the Present Data with the FDB correlation, eqs. (5.6) and (5.7) for 5% ethylene glycol solution, at two flow velocities

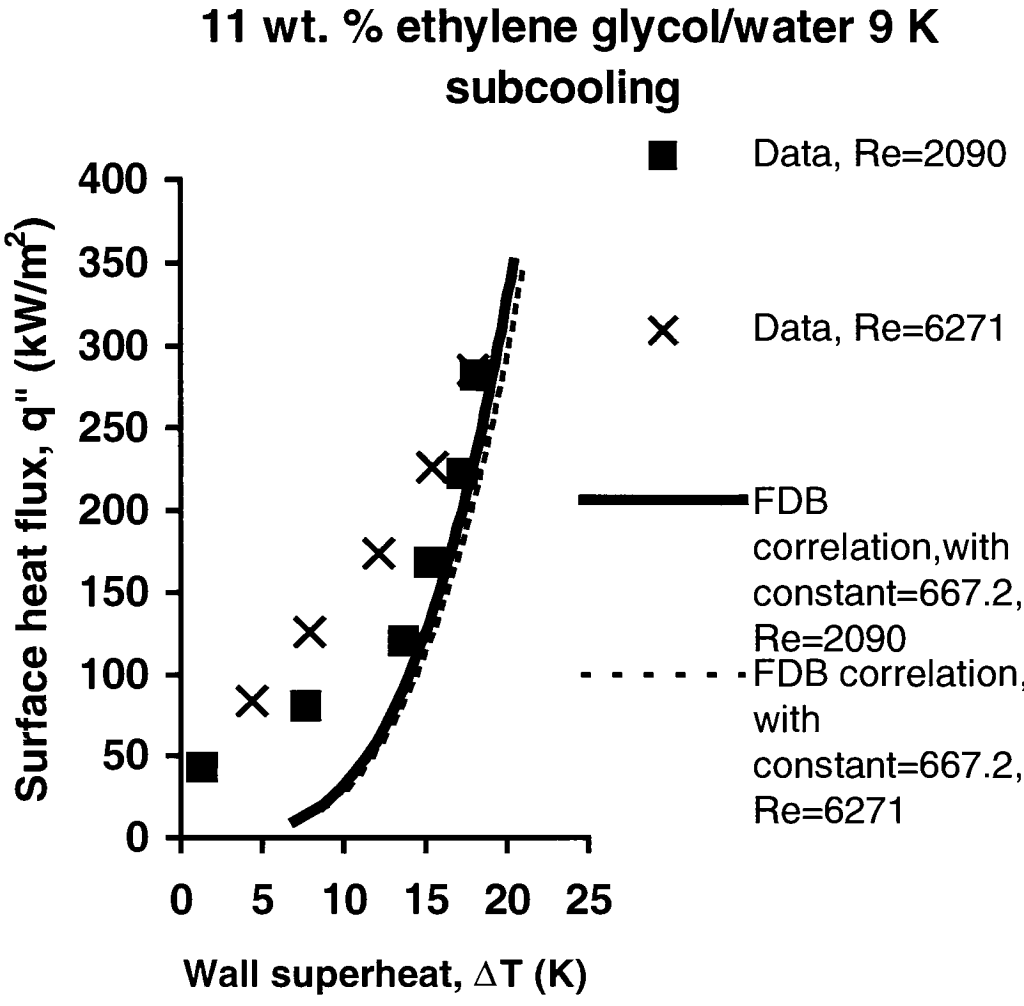

Figure 5.13 Comparison of the Present Data with the FDB correlation, eq. (5.7) for 11% ethylene glycol solution, at two flow velocities

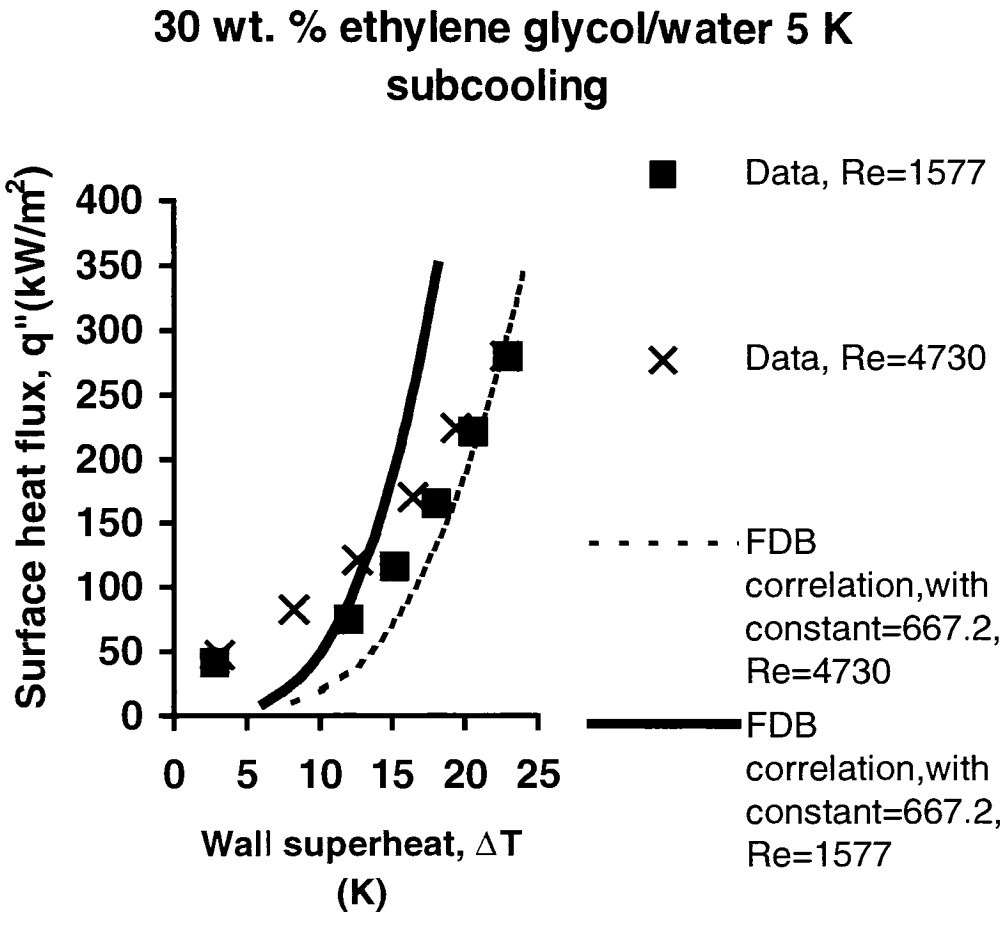

Figure 5.14 Comparison of the Present Data with the FDB correlation, eq. (5.7) for 30% ethylene glycol solution, at two flow velocities

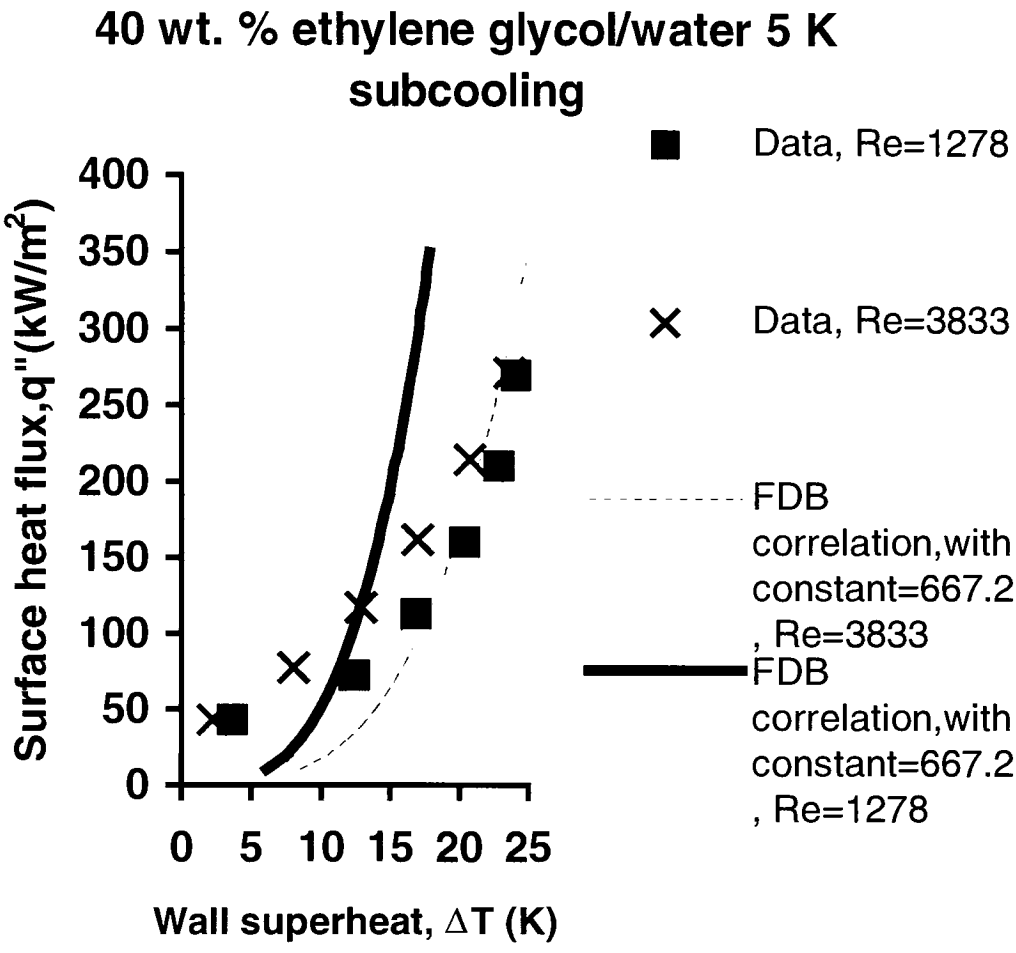

Figure 5.15 Comparison of the Present Data with the FDB correlation, eq. (5.7) for 40% ethylene glycol solution, at two flow velocities

After plotting results from experimental data and for FDB correlation by using eqs.(5.6) and (5.7), the following results are obtained.

Fig.(5.11) shows the results or pure water using the eq.(5.6). It can be seen from Fig.(5.11) that as the wall temperature increases, the heat transfer approaches for both velocities the fully developed boiling for eq.(5.6) asymptotically. Therefore, the agreement for pure water is very good for Re=7339 and 2446.

Fig.(5.12) shows the results for 5 % ethylene glycol concentration. The data shows in Fig.(5.12) that as the wall temperature increases for two velocities, the prediction for Re=6887 by using eq.(5.7) is close because the data and FDB correlation merges. On the other hand by using eq.(5.6), the prediction for Re=6887 is not applicable.

Fig.(5.13) shows the experimental results and FDB correlation for 11 % ethylene glycol concentration. The data and FBD correlation indicate a good agreement for Re=6271 and 2090 by using eq.(5.7) asymptotically.

Fig.(5.14) and (5.15) show the experimental data for 30% and 40% concentration. It can be seen from Fig.(5.14) and (5.15) that the data merges into the FDB correlation by using eq.(5.7) asymptotically.

6. CONCLUSION AND FUTURE WORK

The effect of binary mixtures on flow boiling heat transfer was evaluated experimentally with subcooled flow of water and ethylene glycol mixtures at atmospheric pressure. The results with 0-0.4 ethylene glycol mass fraction were studied. On the basis of the present study, the following conclusions are drawn

1. An experimental study is conducted to study the flow boiling heat transfer of aqueous ethylene glycol solutions. Experimental results are obtained for surface heat flux as a function of wall superheat by systematically varying the mass concentration of ethylene glycol in the range of 0 to 40%. The flow configuration is a rectangular flow channel 3 mm x 40 mm c/s with a circular heater of 9.5 mm diameter.
2. The results for flow boiling of pure water in the fully developed boiling range are in excellent agreement (Fig.(5.11)) with the Kandlikar (1998a) model. This indicates that the flow boiling model for circular tubes is applicable to the present rectangular channel geometry state which parameters in (5.6) and (5.7) were independent of geometry.
3. As the concentration of ethylene glycol increases, the heat transfer performance deteriorates, and becomes dominated by convective effects. The deterioration is seen even for 1% solution.
4. The experimental data is in good agreement with the predictions from the fully developed boiling correlation, eq. (5.7) derived by Kandlikar (1998c) for the convective boiling dominant region.

5. Further work is warranted to determine accurate values of the fluid-dependent parameter F_{fl} for ethylene glycol.

6. Future experiments should focus on higher wall superheats and higher concentrations of ethylene glycol to quantify the diffusion effects in the entire range of concentration.

References

Alves, C, L., 1997" An investigation of the heat transfer suppression mechanisms in the pool boiling of aqueous solutions of ethylene glycol," M.S. Thesis, ME Department, Rochester Institute of Technology, Rochester, NY.

Ambrogi, G, McAssey, E.V., Cozzone, G., Hoover, C., 1997,"The Effect of Off-Design Operation on the Thermal Performance of Propylene-glycol and Ethylene-glycol Engine Coolants," SAE Paper No. 971827, Vehicle Thermal Management Conference, Indianapolis, IN.

Bhowmick, S., Branchi, C., McAssey, E.V., and Gollin, M., 1996, "Heat Transfer Performance of Engine Coolants Under Subcooled Boiling Conditions," ASME ICE-Vol. 26-2, 1996 Spring Technical Conference.

Bhowmick, S., Branchi, C. McAssey, E.V., Gollin, M. and Cozzone, G., 1997, "Prediction of Heat Transfer in Engine Cooling Systems," Proceedings of the 4th World Conference on Experimental Heat Transfer, Fluid Mechanics, and Thermodynamics, Brussels, Belgium.

F.Bosnjakovic., 1930, "Verdampfung und Flussigkeitsuberhitzung", *Tech. Mech. Thermo-Dynam. Berl.* 1, pp.358-362.

P.J. Bruijn., 1960, "On the asymymptotic growth rate of vapour bubbles in superheated binary liquid mixtures", *Physica,'s Grav.* Vol.26, pp.326-334.

Chen, J.C., 1966, "A Correlation for Boiling Heat Transfer to Saturated Fluids in Convective Flow," Industrial and Engineering Chemistry, Process Design and Development, Vol. 5, No. 3 pp.322-329.

Finlay, I.C., Boyle, R.J., Pirault, J.P., and Biddulph., 1987,"Nucleate and Film Boiling of Engin Coolants Flowing in a Uniformly Heated Duct of Small Cross Section," SAE Technical Paper Series 870032.

Forster, H.K., and Zuber, N., 1954,"Growth of a vapor bubble in superheated liquid,"*Journal ofApplied Physics*, vol.25, pp.474-478.

Howell, M., 1996," Investigation of nucleation and heat transfer during subcooled flow boiling on augmented surfaces," M.S. Thesis, ME Department, Rochester Institute of Technology, Rochester, NY.

HYSIM, Version 6,1996, Hyprotech Ltd., Alberta, Canada.

Kandlikar, S.G., 1990,"A general Correlation for Saturated Two-Phase Flow Boiling heat Transfer Inside Horizontal and Vertical Tubes," ASME Journal of Heat Transfer, Vol.112, pp.219-228.

Kandlikar, S. G., 1998a, "Heat Transfer and Flow Characteristics in Partial Boiling, Fully Developed Boiling, and Significant Void Flow Regions of Subcooled Flow Boiling," ASME Journal of Heat Transfer, Vol. 120, 395-401.

Kandlikar, S. G., 1998b, "Boiling Heat Transfer in Binary Systems: Part I - Pool Boiling," ASME Journal of Heat Transfer, 380-387.

Kandlikar, S. G., 1998c, "Boiling Heat Transfer in Binary Systems: Part II - Flow Boiling," ASME Journal of Heat Transfer, 388-394.

Kandlikar,S.G.,1997, "Boiling Heat Transfer Binary Mixtures Part II-Flow boiling in Plan Tubes," *National Heat Transfer Conference*, Vol.4, pp. 27-34.

Kandlikar, S.G., Bijlani, C.A., and Sukhatme, S.P., 1975,"Predicting the Properties of R-22 and R-12 Mixtures-Transport Properties", *ASHRAE Transactions*, Vol.81, Part 1, pp.266-284.

Kandlikar, S.G., and Spiesman, P.H., "Effect of Surface Characteristics on Flow Boiling Heat Transfer," paper presented at Convective Flow and Pool Boiling Conference, Isree, Germany, May 1997

Marto, P.J., Moulson, J.A., and Maynard, m.D., 1968, "Nucleate Pool Boiling of Nitrogen with Different Surface Conditions," *J. Heat Transfer, Trans. ASME*, Vol.90, pp.437-445.

McAssey, E.V., and Kandlikar, S.G., 1999, "Convective Heat Transfer of Binary Mixtures under Flow Boiling Conditions," Paper to be presented at the International Conference on Two-Phase Flow Modeling and Experimentation, Pisa, Italy.

McAssey, E. V., Stinson, C., and Gollin, M., 1995, "Evaluation of Engine Coolants Under Flow Boiling Conditions," Proceedings of the ASME Heat Transfer Division, HTD-Vol. 317-1, p. 193-200.

Mizo, V., 1995," Investigation of bubble departure mechanism in flow boiling using high-speed photography,"M.S. Thesis, ME department, Rochester Institute of Technology, Rochester, NY.

Plesset, M.S., and Zwick, S.A., 1954, "The growth of vapor bubbles in superheated liquids," *Journal of Applied Physics*, vol.25, pp.493-500.

Rayleigh, Lord, 1917,"On the pressure developed in a liquid during the collapse of a spherical cavity," *Philosophy Magazine*, vol.34, pp.94-98.

Raykoff, Taavo, 1996,"Bubble growth rate and heat transfer suppression in the flow boiling of binary mixtures," M.S. Thesis, ME department, Rochester Institute of Technology, Rochester, NY.

Scriven, L.E., 1959,"On the dynamics of phase growth," *Chemical Engineering Science*, vol.10, pp.1-13.

Spiesman, P.H., 1997,"Effect of Surface Characteristics on Flow Boiling Heat Transfer,"M.S. Thesis, ME Department, Rochester Institute of Technology< Rochester, NY>

Stumm, B.J., 1995,"investigation of bubble departure in subcooled flow boiling of water,"M.S. Thesis, ME Department, Rochester Institute of Technology, Rochester, NY.

Van Stralen, S.J.D., 1967," The growth rate of vapour bubbles in superheated pure liquids and binary mixtures/ Part I: Theory," *International Journal Of Heat and Mass Transfer*, Vol. 11, pp.1467-1489.

Van Stralen, S.J.D., 1967,"The growth rate of vapour bubbles in superheated pure liquids and binary mixtures/ Part II: Experimental results," *International Journal of Heat and Mass Transfer*, Vol. 11, pp.1491-1512.

Vignes, A., 1971,"Diffusion in Binary Solutions," Industrial and Engineering Chemistry Fundamentals, Vol.5, pp.189-199.

Wilke, C.R., and Chang, P., 1955,"Correlation of Diffusion Coefficients in Dilute Solutions," AIChE Journal, Vol.1, pp.264-270.